TAMPEREEN TEKNILLINEN YLIOPISTO
TAMPERE UNIVERSITY OF TECHNOLOGY

Mika Töhönen

Piezoelectric Vibration Damping of Rolling Contact

Julkaisu 1362 • Publication 1362

Tampere 2015

Tampereen teknillinen yliopisto. Julkaisu 1362
Tampere University of Technology. Publication 1362

Mika Töhönen

Piezoelectric Vibration Damping of Rolling Contact

Thesis for the degree of Doctor of Science in Technology to be presented with due permission for public examination and criticism in Konetalo Building, Auditorium K1702, at Tampere University of Technology, on the 30th of December 2015, at 12 noon.

Tampereen teknillinen yliopisto - Tampere University of Technology
Tampere 2015

ISBN 978-952-15-3669-4 (printed)
ISBN 978-952-15-3709-7 (PDF)
ISSN 1459-2045

Abstract

Machines, which contain heavy rotating objects like rolls, are always sensitive to vibrations. These vibrations can usually be limited by a conservative design approach, by carefully balancing the rolls and by applying high precise manufacturing techniques. More critical are machines, in which rolls are in direct rolling contact and a web-like thin material is fed through this contact. Such material manipulation is used for example in manufacturing of paper, thin foils and metal sheets or in rotary printing machines. In the first case the rolls today are covered by polymer materials in order to make the contact zone larger. This produces non-classical delay type resonances, when the roll cover is deformed in the contact zone, and this penetration profile is entering the contact zone again before complete recovery. This type of self-excited nonlinear vibration is difficult to control with purely traditional damping methods. Active damping methods bring more possibilities to adapt to different running conditions. The knowledge of existing delay-resonance cases calls for methods, actuators and control circuits, which have the required performance to move rolls of *10* tons mass at frequency band *100 Hz* and peak-amplitude level *0,01 mm*. After closing out many other possibilities, piezoelectric actuators have been proposed to such damping task and the purpose of this thesis is to evaluate the feasibility of commercially available actuators in this service.

Piezoelectric actuators are very promising for vibration control applications, because of their easy controllability, high performance in producing large magnitude forces in combination with small magnitude motion outputs in an extremely fast response time. The control is straightforward by simply variating the input voltage of the actuator. Classical damping approaches are bringing the possibility to utilize large control gains in a wide stability domain. When control voltage is generated based on the vibration data measured from the system, which is the case in active damping approach, a counter-force driven by the piezoactuator can be fed in the opposite phase to the vibrating system. It is also possible to build a passive vibration damper by connecting an electric circuit to the electrodes of the piezoelectric actuator in order to harvest the

electric energy originating from the oscillating mechanical part of the system. These electric circuits can consist of a resistor, an inductor and a capacitance in different serial or parallel layouts. In order to make such circuit adaptive one, sophisticated control electronics is needed to on-line modify the adjustable circuit parameters.

Preface

The research work has been mainly carried out in the former Laboratory of Machine Dynamics at Tampere University of Technology during the time frame 2005-2007 in the research project SMARTROLL – Dynamics and Control of Direct Drive Rolls under the financial support of the Finnish Funding Agency for Innovation (Tekes). The other research partners in the work have been the University of Oulu and Karlsruhe Institute of Technology (KIT) while the industrial financiers have been Metso Paper Inc., ABB Pulp and Paper Drives and Stora Enso Fine Paper, Oulu mill. I am grateful for the Graduate School of Concurrent Mechanical Engineering funded by the Ministry of Education for accepting me to the PhD program as a graduate student. I also like to thank the Eemil Aaltonen Foundation for funding the work.

I wish to express my gratitude to my supervisor Professor Erno Keskinen for the inspiration and guidance during this study. I like to thank him for helping to create a flexible and productive working environment and for the encouragement and support during the latter stages of writing the manuscript. I like to thank Docent Juha Miettinen for his effort and participation during the work as well as Dr. Pekka Salmenperä for his help with the measurements. I would also like to thank Professor Wolfgang Seemann for his guidance during my academic year in Karlsruhe as well as his comments and language checking that helped to improve the quality of the manuscript. In addition a great thank to the staff of former Department of Mechanics and Design for having a pleasant and supportive working environment.

The assessors of the manuscript, Professor Arend Schwab from the Delft University of Technology and Professor Robert Hildebrand from the Lake Superior State University, Michigan are kindly acknowledged for their valuable comments to improve the manuscript. I also appreciate their effort to carry out the review in a short time period.

I like to thank my current colleagues in Structural Analysis and Hydrodynamics group at Technip Offshore Finland for their support. Special thanks to my friends who helped to widen my perspectives and to relax at my free time.

I would like to specially thank my parents Alli and Raimo for the steady support and encouragement which has been helpful and important. Finally, I wish to express my warmest gratitude to my dear Heidi for the love, patience and support during the course of this work. I dedicate this thesis to my sweet daughter Senja.

Nokia, December 2015

Mika Töhönen

List of contents

Nomenclature

A_p	pressure area at plus chamber of hydraulic cylinder
a,b,c	factors in elastic nip contact model
B	bulk modulus of fluid
$\boldsymbol{C}$	damping-resistance matrix of piezoelectric damped system
$\boldsymbol{c}$	damping matrix of two-roll system
C_{ex}	electric capacitance in RLC circuit
c	damping coefficient of oscillator
c_1	damping coefficient of upper bearing
c_n	nip damping
C_p	electric capacitance of piezoactuator
d_{33}	strain constant of piezoelectric material in the direction of applied voltage
E	elastic constant
F	force in spring equation of piezoactuator
F_e	amplitude of harmonic excitation force
F_d	desired nip load
f	rotational frequency of polymer roll
f_e	time-dependent excitation force
f_n	running frequency of roll at delay-resonance with n stripes in the polymer cover
f_o	natural frequency of roll stack in roll-against-roll mode
F	hydraulic actuator force
g	acceleration of gravity
H_p	electromechanical force coefficient of piezoactuator
h	roll cover thickness
$\boldsymbol{K}$	stiffness-capacitance matrix of piezoelectric damped system
$\boldsymbol{K}_n$	stiffness matrix of nip elasticity in piezoelectric damped system
$\boldsymbol{k}$	stiffness matrix of two-roll system

$\boldsymbol{k}_n$	stiffness matrix of nip elasticity in two-roll system
K_a	combined structural stiffness of piezoactuator
K_D	gain in the derivative part of controller
K_p	gain in the proportional part of controller
k	spring constant of oscillator
k_1	stiffness of upper bearing
k_h	constant of hydraulic spring
k_n	nip stiffness
k_p	mechanical stiffness of the ceramic core of piezoactuator
k_s	stiffness of the metallic casing of piezoactuator
L	inductance of L part in RLC circuit
ℓ	length of nip line
$\boldsymbol{M}$	mass-inductance matrix of RLC circuit damped system
$\boldsymbol{m}$	mass matrix of two-roll system
m	mass of oscillator
m_1, m_2	mass of upper and lower roll
N	nip load
n	integer number
$\boldsymbol{n}$	unit load vector in piezoelectric damped oscillator model
Q	electric charge in RLC circuit
q_p	electric charge in piezoceramic actuator
R	electrical resistance in R part of RLC ciecuit
R_1, R_2	radii of rolls in contact
r	force magnification factor in nip loading mechanism
T	revolution time of roll, time delay in nip
T_e	time period of one excitation oscillation
t	time
$\boldsymbol{U}$	complex amplitude vector of piezoelectric damped oscillator
u	control input to proportional valve

$\boldsymbol{u}$	state vector of piezoelectric damped oscillator
u_e	applied external voltage
u_p	voltage over piezoelectric actuator
v	paper web line speed
w	weight per length
x	displacement, axial displacement of piezoelectric stack actuator
$\dot{x}$	velocity of piezoelectric damped oscillator
$\boldsymbol{x}$	state vector of roll system in classical control approach
x_d	desired displacement
$\dot{x}_d$	desired velocity
x_1	displacement of upper roll
x_2	displacement of lower roll
$\boldsymbol{y}$	state vector of piezoelectromechanical system in RLC shunt circuit approach
z	shape excitation
Z	amplitude of shape excitation
α	piezoelectric coupling coefficient
β	average curvature of rolls in contact
δ	compression in cover
ε	cover penetration
η	viscosity of polymer
γ	time delay factor
τ_r	time constant in cover recovery
ω	resonance angular frequency of RLC circuit
Ω	angular frequency of excitation
θ_1, θ_2	angular position of upper and lower roll
λ	wave length in web thickness variation
χ	complex time delay function in frequency response solution of damped nip system

ψ	angular coordinate at roll surface

CD	machine Cross Direction
DE	Drive End of roll
FRF	Frequency response function
MD	Machine Direction, direction of material flow through nip
TE	Tender End of roll

1. Introduction

1.1 Background and motivation

Rolling contact is a common solution in industrial web handling processes in the production of paper, steel and aluminium folia. A typical arrangement has two rolling cylinders, between which the web is fed to get the required surface manipulation during the short period the web is in the contact zone. As the metal-against-metal contacts are leading to too narrow contact zones and correspondingly to too short manipulation times for softer web materials like paper, non-metallic elastic covers have been introduced for at least one of the member rolls in the contact. The resulting broader contact nip brings better performance for the calendering and the coating processes by means of a longer web manipulation time allowing the mill to use higher running speeds. Typical lay-outs of calendering and coating units with covered rolls in the dry end sections of the paper production line are shown in Figure 1.

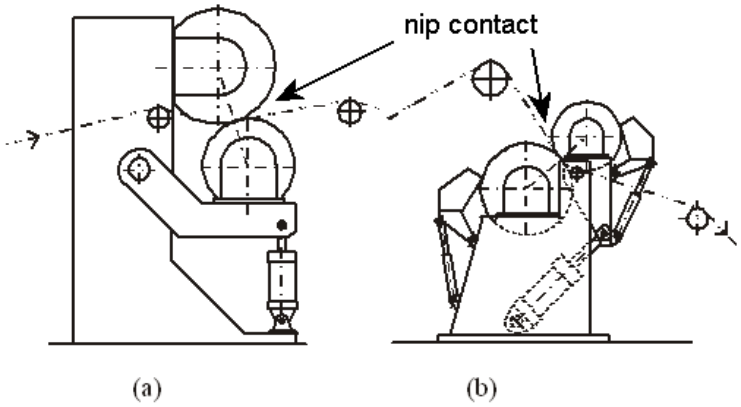

Figure 1. Calendering (a) and coating (b) units with polymer covered rolls in paper production.

At higher running speeds, however, instabilities in the rolling contact appear disturbing the production and thus cutting the annual output of the production line. Such instability is forcing the rolls in an oscillatory motion in the direction normal to the contact surface, which is finally marking the web by cross-directional stripes (Kustermann 2000). This phenomenon is a consequence of the well known property of the viscoelastic cover polymers to slowly recover after transient compression

deformations (Ward 1993, Vuoristo 2002). This unwanted phenomenon has been widely investigated, the result of which is a common agreement among the researcher society about the leading instability mechanism. A simple and exact rule is predicting the unstable and stable running speeds (Hermanski 1995), but the threshold speed, above which the phenomenon called as delay-resonance will be initialized in a particular system configuration is less clear, as it depends on the dynamic balance between the negative and positive damping energies fed to the system. Based on measurements (Salmenperä 2013), the response behaviour of nip systems is a complex one, because (1) the polymer cover brings a delay-effect, (2) long rolls behave like thin-walled elastic circular cylindrical shells and (3) the loading circuit is contributing to the motion as well. This is the reason why no clear dimensioning rules or stability charts have been published yet. Paper industry has a strong interest to overcome this difficulty, which in worst cases may reduce the production rate significantly.

Academic research teams have been involved to the solution process of such cases, when they simultaneously appeared in the late 90's at high speed production lines in several machine start-ups everywhere in the pulp and paper industry. As a result of an extensive research, a set of different approaches has been introduced to control nip oscillations. They can roughly be classified to passive, semi-active, active and smart approaches. Passive ways are based on a fixed set of mass, stiffness and damping parameters in the primary system, while in semi-active ways this parameter set of an additional secondary system can be tune and slide during the run. Smart approaches are based on an on-line identification of stable and unstable regions to find an acceptable running window. Some limitations and related difficulties are reducing the performance and the return of investment of these developments making it necessary to have a look to the last not completely investigated way, which is the active damping approach.

The active fluid powered damping circuits have been successfully connected to the bearing housings of the rotating systems to stabilize whirling motion driven by unbalance forces. When unstable nip oscillations represent one or two decade higher frequency domains, the performance of rather slowly reacting fluid powered actuators is not enough for this application. This limitation has led to the investigation of an

approach, in which active control algorithms have been applied to drive a servo loop consisting of a secondary piezoelectric actuator installed parallel with the primary fluid power actuator pressing the rolls together.

1.2 Objectives and related research questions

The main objective of this thesis is to evaluate the feasibility of the piezoelectric actuators for active damping of nip oscillations in rolling contact. To reach this knowledge the following tasks have to be carried out: (1) a theoretical analysis, (2) build of a set-up and (3) a performance evaluation of the damping circuit.

(1) The first objective is to reach the state-of-art level in the research field by means of theoretical and literature based analysis of piezoelectric damping circuits in various academic set-ups and industrial applications. Based on this knowledge, different system lay-outs to connect the piezoactuator mechanically and electrically to the existing roll press will be proposed.

(2) Based on the theoretical analysis, a design of the actuator circuit will be developed, fabricated and installed to the existing pilot roll press, whose response behaviour exhibits nip oscillations with a similar character of a typical delay-resonance case.

(3) To evaluate the damping performance, the piezoelectric damping circuits will be analyzed by system level modelling and analysis and by measuring the response behaviour of the set-up added to the pilot roll press.

In order to reach the objectives, the following fundamental research questions related to the circuit, actuator and algorithm solutions have to be answered:

(1) *Which mechanical interfaces and circuit arrangements are able to compensate the oscillatory motion in an effective way ?*

(2) *Which phenomena are controlling the transmission of external damping energy to the system ?*

(3) *Which control principle brings a sufficient performance in damping the delay-resonance oscillation ?*

By knowing that the original system under investigation is already a complicated arrangement of polymer covered rotating structures and fluid powered loading mechanisms, any additional sub-system will increase the complexity level of the entire system bringing also the difficulty to find stable enough control solution.

1.3 Contributions

The main purpose of this research work has been to develop a damping system based on piezoelectric actuators to control vibrations appearing in rolling contact situations in the paper industry. The research work has been divided to theoretical and experimental parts. The theoretical part includes a comprehensive review on piezoelectric damping methods in various academic and industrial applications. The most promising piezoelectric actuator circuits, including classical controllers and external RLC-circuits, have then been selected to deeper evaluation by means of computer simulation in the time and frequency domains. The results of this analysis have then been utilized in the experimental part of the work consisting of design and build of the actuator interface on the top of an existing pilot roll press representing a design scaled to the half size of a corresponding industrial production unit. This hardware platform makes it possible to realize different active, semi-active and passive piezoelectric damping circuits, from which the one based on the direct

velocity feedback mode (the classical D-controller approach) has been finally chosen to the complete implementation and testing phases.

The following original contributions were developed in the course of the work:

(1) Development of two different circuit arrangements for active damping of nip oscillations of polymer covered rolls by parallel piezoactuators: (1) the classical controller approach, and (2) the passive RLC shunt circuit.

(2) Design and implementation of the parallel piezoelectric actuator circuit for the pilot roll press.

(3) Numerical and experimental evaluation of the performance of the active damping system in different circuit arrangements.

2. Theoretical background

2.1 Vibration damping of rolling systems

Rolling systems are sensitive to vibrations, because any imperfections in the contact interface or in the mass distribution of the rotating parts may easily excite the system to oscillations by means of a displacement or a force controlled input mechanism. When such disturbances have a great influence to the production rate of many industrial processes, the research activity for finding economical and technically working solutions has been both wide and deep. This chapter brings a review about what has already been done and reported, but also what research lines are still waiting to be opened and evaluated.

2.1.1 Systems and phenomena

There are many processes in the industry, where circular rotating components are pressed together in order to modify the web material thinner, smoother or to add a film or a coating. This review is limited to roll presses in the paper industry with particular interest to dry end sections in paper production and finishing lines.

According to many observations, the two most vibration sensitive variations of roll press are the coating unit and the calendering unit (Figure 1) (Bradford 1988, Emmanuel 1985, Parker 1665, Shelley 1997).

A coating unit based on the film sizing principle (Lehtinen 2000) has one or two application boxes (Figure 1b), which by making use of a rotating rod are spreading the coating pasta on to the surface of one or on both of the two member cylinders to be fed to the nip zone and pressed on the surface of the paper web. To get enough time for the mass transfer of the coating into the web, one cylinder is polymer covered while the other cylinder is a hard one. This arrangement actually forces the harder cylinder to penetrate into the elastic cover of the soft cylinder.

A similar situation is present in the calendering process (Figure 1a) but with elevated temperature and one decade higher line load and peak pressure for effective polishing of the paper web (Jokio 1999).

Soft nips became popular in the late nineties' when significantly improving the nip manipulation process and making it possible to use higher running speeds. In contrast to many success stories, reports about difficult nip oscillation problems were also common after start-ups and speed-upgrades. The common nominator in these experiences was the unexpected and complex response of the polymer cover (Keskinen 1998). It looked like the speed of the line, the nip width, the time constant of the viscoelastic cover polymer and the eigenfrequencies of the roll stack were sliding to domains, where new-type of instabilities totally different from the classical resonance states, were appearing without a warning (Chinn 1999, Filipovic 1997, Sueoka 1993).

Two dominating time constants can be identified in the cover deformation dynamics. The first is the pulse time controlling the duration time of the cover material particles passing the compression zone in the nip. The second one is the revolution time of the roll, which is controlling the frequency, how often each material particle of the cover is travelling through the nip. As polymer covers are made of viscoelastic materials, they respond to excitation in a complicated way. During the pulse time the cover material is under the effect of a displacement-controlled relaxation phase while the two decades longer revolution time (minus the pulse time) represents the free-recovery period (Ward 1993).

So far, as the rolling process is running smoothly in steady-state conditions, there is no source for oscillations. The stationary situation is disturbed, if for any external or internal reasons (Keskinen 2000), the rolls are forced to a relative translatory motion in the direction normal to the contact surface. A typical external excitation is the periodic thickness variation of the paper web entering the nip, a situation which appears in Figure 2a.

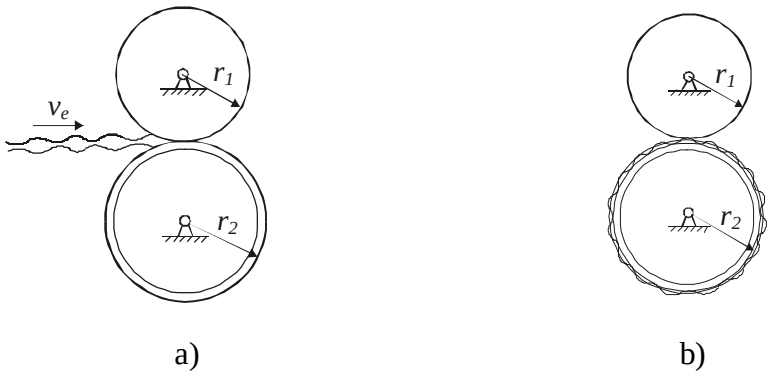

Figure 2. Excitations forcing the rolls in nip oscillation: a) external web thickness variation and b) internal cover barrel profile, which can be also a consequence of a run at delay-resonance speed.

The consequence of such motion is that the hard roll will mark the cover of the soft roll by a shape profile corresponding to the relative motion history. Following from the viscous property of the cover polymer, closer to the leaving edge of the nip, the deformation profile is higher, but closer to the entering edge, it is getting lower. This attenuation is driven by the recovery dynamics of the polymer. The more there is time-delay between two successive nip passes, the better the profile from the previous nip phase is cleaned before the next nip entry. On the other hand, if the roll revolution time is getting shorter, which is the case at higher running speeds, the more information from the previous nip history is brought to the nip again and again. This can finally initialize self-excited vibrations if two conditions are filled: (1) the speed is constant and above certain critical threshold speed and (2) the speed has such a value that an integer multiple of the running frequency f has an exact match with the natural frequency f_o of the roll system in relative roll-against-roll oscillation mode, $nf = f_o$. This leads to a discrete spectrum of rotation frequencies, $f_n = f_o/n$, at which the system can be in delay-resonance. The corresponding speeds are called delay-resonance speeds, because they are driven by the delay effect of the roll cover (Vinicki 2001, Yuan 2002). If the conditions for such nip vibrations are favourable over a sufficient long duration time, the roll cover finally gets a barrel profile (Figure 2b), which in turn takes the role to be an internal excitation source at any new speed window the roll stack will be run (Salmenperä 2013).

The vibration modes of a roll system are similar to the ones of a system with two masses interconnected by a spring and supported to the fixed reference by two more springs. The lower of the two modes represents the synchronous motion of the rolls while the other higher one exhibits the unwanted non-synchronous roll-against-roll mode. For different roll masses and support springs these modes are more or less mixed ones. When the lower eigenfrequency is in the same scale with the rotation frequency, the web marking with a rather long wave length and a weak visibility has less interest as compared with the sharp stripe profile taking place at the higher frequency.

If the nip oscillation can continue at delay-resonance state, the roll cover is finally marked by a barrel profile of parallel stripes (Kustermann 2000). Such profile has some permanent component also, which can not recover freely at any finite time. Because this marking is representing the eigenfrequency of the roll system, it then follows an interesting phenomenon. If the running speed is modified in the neighbourhood of the delay-resonance speed, the earlier marked profile takes an excitation role starting forced vibration at a modified frequency. When, simultaneously the system in the background still vibrates at the original eigenfrequency, the consequence of this interference is the beating response of the two interacting vibrations (Salmenperä 2013). If the running speed is then slide slowly back and fort in larger running window around the resonance speed, the permanent marking profile can be cleaned almost completely.

If the paper finishing process is driven at speeds, where delay-resonances exist, the smoothness of the paper surface is lost, because the barrel profile of the roll cover and the steady oscillation is marking the web by cross-directional stripes. The only safe way to avoid this serious quality drop is to limit the running speed below the threshold speed. Because this is cutting the production rate, there has been strong pressure to find ways to solve the problem in the first stage theoretically and based on that knowledge in the second stage also technically.

2.1.2 Review of solution methods

Damping of delay-resonances in rolling systems does not differ too much from the damping of classical resonances of passive resonators or rotor dynamic systems. The methodologies can be classified to the following categories:

Passive damping methods
Semi-active damping methods
Active damping methods
Soft computing and smart methods

Passive damping methods

Passive damping methods represent a fixed parameter design. This means that based on a computational vibration analysis, the system parameters will be fixed in the design phase, so that the rotational frequency of the rolls do not meet the natural frequency of the rolls in nip oscillation mode. This principle, which actually avoids imbalance and shape eccentricity driven resonances, does unfortunately not eliminate the possibility of delay-resonances, because they always appear, if any multiple of the rotation frequency has a match with the nip oscillation eigenfrequency, which in turn is the frequency of the delay-resonance (Yuan 2002). When these multiples can not be avoided within the economical production speed range, the only strategy is to add strong enough external damping and/or to go direction heavy design in order to push higher the threshold speed, at which the delay resonances appear. The effect of external dampers is very limited, because the amplitude level of displacements even in difficult delay resonances oscillations can be counted in units 10^{-5} *m*. The heavy design principle leads to a conservative and expensive dimensioning of the load carrying parts and foundations, which is increasing the infrastructure costs of the production lines.

Semi-active damping methods

These methods are tailored for systems sensitive to delay-resonances. They are different variations from the principle to add a classical dynamic mass damper (den Hartog 1947) on the top of the system. When the classical damper is normally tuned to a fixed eigenfrequency or to a fixed excitation speed, the situation in delay-resonance case in a roll press is much more challenging. The first problem is that the eigenfrequency is not constant, because it depends on the line load level, and on the temperature and age of the polymer cover (Salmenperä 2013). The second difficulty is the sliding of the running speed. When the delay-resonance is locked to the eigenfrequency of the nip oscillation mode, the most promising way is to make a tuning to exactly to that frequency. Automatic self-tuning algorithm is still needed to tackle the wandering phenomenon of the eigenfrequency.

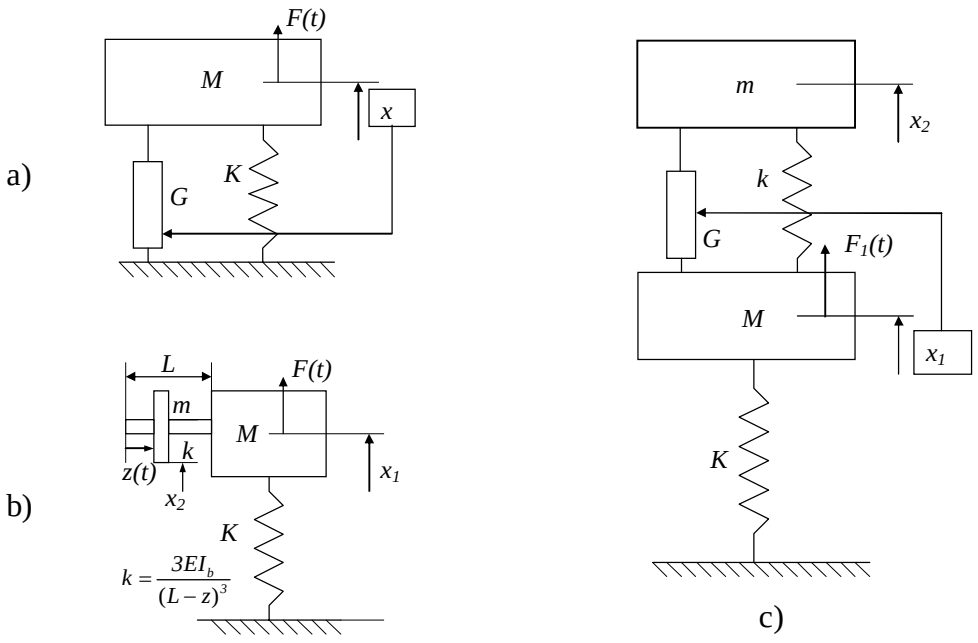

Figure 3. An active vibration damper (a) and two tuned modifications of the semi-active dynamic mass damper based on a travelling disk on a screwed shaft (Karhunen 2005) (b) and on adjustable gains in a piezoactuator driven secondary mass (Virtanen 2006) (c).

Practically this means that the eigenfrequency of the mass damper has to be on-line fixed to the identified nip oscillation eigenfrequency. Such tuning can be done for instance by moving a concentrated mass on the span of a cantilever beam for modifying the eigenfrequency of this beam system to match the frequency of delay-resonance illustrated in Figure 3b (Karhunen 2005).

Another realization of the semi-active damper is based on the use of a piezoactuator as shown in Figure 3c. A concentrated secondary mass is suspended by such an actuator, the effective stiffness of which is modified by updating the proportional gain in the position control loop. This arrangement makes it possible to on-line tune the dynamic mass damper to exactly match the delay-resonance frequency. The tuning becomes less critical, if the derivative gain is used also to bring velocity feedback in the damping (Virtanen 2006). One more modification of the piezoceramic dynamic mass absorber is based on the on-line identification of the resonance frequency. The mass damper is then forced to vibrate harmonically in direction opposite to the oscillation of the bearing housing, on which it has been mounted. The amplitude of this counter-oscillator is modified until the motion of the bearing housing is limited enough.

Active damping methods

Such damping principles require the use of high performance actuator circuits, whose frequency band is covering well the predicted delay-resonance frequencies. Many investigations show that the fluid power actuators, which are used as primary actuators for the nip loading purposes, are not fast enough to serve as vibration dampers (Virtanen 2006). In contrast to that, piezoceramic actuators driven by computer controlled voltage source, have the required performance on large frequency band covering easily nip oscillation spectrum (Colla 2008). Active dampers, like the one in Figure 3a, can be mounted between the non-moving reference and the bearing housing of the lower one of the member rolls so that the additional actuators are parallel with the main actuators used for line load control of the roll nip. Better performance is still obtained by installing the actuators between the bearing housings of the member rolls, which makes it possible to feed or absorb mechanical energy directly to and from the oscillatory system.

There are mainly four different approaches to apply the active vibration concept. The first approach is just to add strong damping by making the use of large derivative gain in the feedback loop, which is bringing to the piezoactuator the role of an artificial viscous damper (Preumont 1997). The control principle is actually to direct the relative speed between the bearing housings to be zero. Such velocity feedback can be updated to include artificial stiffness by means of an adjustable proportional gain. The control principle is then based on the compensation of the relative displacements between the bearing housing. Such PD controller can be further extended to include the acceleration gain and feedback delays bringing more possibilities in tuning the damper (Fuller 1996). When the roll system actually represents a multi-degree-of-freedom system, the general approach is called the state variable control as it utilizes completely the observed system state. The fact that a piezoactuator is a transducer between mechanical and electrical sub-systems makes it possible to feed the mechanical vibration energy out from the system to be damped in an external electrical circuit by means of resisting elements. The third possibility is to process the frequency content of the relative motion and generate a counter movement to compensate that motion. Such approaches are, however, sensitive to instabilities as the measurement information is recorded under the effect of the controller itself.

Finally, as a fourth approach, an RLC-circuit connected to the electrodes of the piezo-actuator can be adjusted by a shunt to transform the mechanical motion of the actuator to the oscillatory current over the resistance (Preumont 1997, Hagood 1991). The solenoid and capacitor in the circuit bring some tuning possibilities to better adapt to the frequency band typical for delay-oscillations in nip.

Soft computing and smart methods

This approach is based on the knowledge that delay-resonance states exist when the multiple of the roll rotation frequency is matching with the eigenfrequency of nip oscillation. This rule actually generates a discrete spectrum of corresponding delay-resonance speeds, on which there is a potential risk to fall in the resonance state. This knowledge can now be utilized in supervising the system to be run only at accepted narrow stable running windows between the successive avoidable unstable resonance

speeds. As the spectrum depends on process parameters like line load, the eigenfrequency has to be on-line identified to correctly build the rule basis. This approach has been successfully implemented to the existing pilot roll press (Salmenperä 2013), where no other reasons are setting requirements for the running speed. In industrial production lines, however, the rule-based running speed setting may lead to conflicts as neighbouring sections in the same machine line can have individual resonance frequencies and individual speed constraints.

2.2 Piezoelectric actuators in vibration control

2.2.1 Introduction

Piezoelectric actuators are used in particular industrial systems and applications representing demanding processes and high technology products. The main applications are in three different areas:

Fast control of small motions in high precise manufacturing and injection processes
Energy harvesting from vibration for power supply of electronic circuits and wireless sensors
Damping of vibrations

High precise applications

This application area is important for car industry, as circular cylinder borings of engine blocks are replaced by oval-shaped chambers and piston cross-sections. The machining of such shapes can be done with machine tools equipped with piezoceramic tool movers on the top of the carriage chain. Fast opening of fuel injection valves in engines is one of the rare mass-production applications. Another example from high precise machining is the compensation motion of the tool to follow the cross-sectional whirling motion of long paper machine rolls during turning and grinding.

Energy harvesting

The second area is becoming important, when wireless sensing and actuating systems are popular in network applications like in environmental monitoring. The energy to be caught is in most cases coming from the background noise making it random and broadband. A typical mechanism is to hang a concentrated mass on the top of a piezoceramic beam-like element, whose other end is fixed to the oscillating base structure. The resulting oscillatory motion is deforming the piezoelement generating a dynamic voltage over the material. Continuous elements are more common in micro scale than stacks, which are more typical structures in macro scale actuators.

Damping of vibrations

Vibration damping by piezoceramic elements is actually the same process as energy harvesting by piezoceramic transducers. The only difference is that the scale is larger and there is usually no need to store the energy or feed power back to the network. While academic research has focused to the vibration damping of continuous structures covered by bonded layers of piezoceramic materials (Moheimani 2006, Zhang 2004), the technical applications are more oriented to the use of linear actuators built of a multilayer stack. Industrial applications of piezoelectric dampers are not common, because the costs of control electronics and precise assembly interface are relatively high for mass production. Due to the high costs, piezoelectric damping is mainly used in high technology products like in wind turbine blades, in composite sport gears, in satellites, in aircraft structures, in defence industry and in chatter damping in machining processes. One of the most important applications is the damping of background noise and transient shocks disturbing the micro-scale positioning tasks in semiconductor industry.

2.2.2 Vibration damping by piezoelectric actuators

A piezoelectric actuator is an excellent device for vibration control applications because of its large force generation, very short response time and easy controllability. Piezoelectric actuators in vibration damping applications can be controlled passively, semi-actively or actively. Some authors (Ahmadian 2001, Barrett 1995) review some control techniques for piezoelectric actuators that have been used in the 1980s and 1990s. They divided control method into three categories: (1) methods that use passive electrical elements to shunt the piezoceramic element, (2) methods that employ an active control system to drive the piezoceramic element, and (3) hybrid and semi-active methods that combine the shunted and the active control techniques.

Good overview of piezoelectric shunt damping circuits and their modelling is given in (Hagood 1991). Different control methods of piezoelectric materials in vibration damping applications are presented also (Niederberger 2005), a reference in which different passive and semi-active shunt circuits are used for vibration damping and noise control applications.

Active vibration control using piezoelectric actuators has been successfully used (Barrett 1995, Simões 2007) to damp rotor-dynamic effects acting on the bearing housings.

2.2.3 Damper interfaces and damping circuits

Piezoelectric damping materials can be continuous material continuums or packed into a compact actuator structure. A typical layout in continuous structures is to bond a layer of piezoelectric material on upper and lower surfaces of a cantilever beam in order to utilize the large strains at the maximum distance from the neutral axis to produce enough compression or extension to the outermost piezoceramic layers, when the beam is bending during vibration (Clark 1998). Correspondingly this arrangement also brings largest bending moment for the layer when stressing it by voltage acting over the piezoceramic layer to produce a damping effect resisting the motion.

A stack actuator (see Figure 4) is built of a large number of circular thin plates in random orientations around the layer normal to produce in the normal direction large enough total displacement and force resultant (Fuller 1996).

The damping principle can be passive or active one in both distributed and in stack actuator cases. The passive damping is based on external shunt circuits, which are connected to the electrodes of the actuating element (Law 1996, Clark 2000). If this circuit has a resisting element only, the damping property is distributed to broader frequency band. By adding an inductance and a capacitance to the circuit, one can make proper tuning by utilizing the resonance state of the RLC-circuit for maximizing the damping at the dominating frequency of the mechanical system, for instance by tuning to the lowest structural eigenfrequency. If the vibration peak is moving for any reason, a synthetic impedance device has to be used to adapt the resonance tuning to the changing structural vibration even in multi-modal vibration cases, which is a semi-active extension of the use of shunt circuits (Adachi 2004, Wang 2002).

In the actively controlled damping approach, a force in opposite phase to the vibration is fed into the system. The principle is to damp vibrations in structure by producing active counter-force with the piezoelectric actuator. Control of piezoelectric actuator is straightforward by direct compensation of the input voltage, which in turn can be generated from the vibration data measured from the system. In literature one can find simple, robust and effective controllers for active vibration damping applications (Fuller 1996, Clark 1998).

3. Piezoelectric damping of single degree of freedom system

Case studies with a simple one degree of freedom model were done in order to monitor the system responses without and with different vibration damping methods by using the piezoelectric actuator. The model consists of a mass connected to a spring and a damper. In later cases a piezoelectric actuator was added to the system in parallel with a serial connection of an inductance, a resistance and a conductance.

3.1 System equations of piezoelectric dampers

3.1.1 State equations of a piezoceramic stack actuator

The core of the piezoactuator is a multilayered stack of a piezoelectric ceramic material, which is brittle and can carry only compressive stresses. This is why the core is in a compressive pre-stress state inside a metallic cylinder, which correspondingly is in a tensional pre-stress state. This arrangement shown in Figure 4 makes it possible to use the piezoactuator in the pulling direction also.

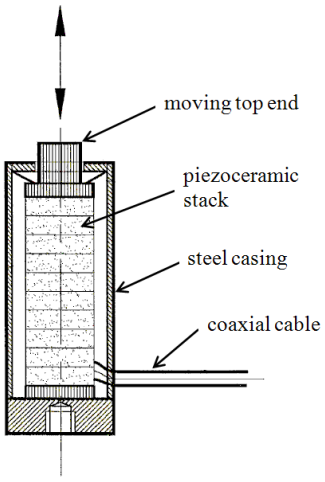

Figure 4. The structure of a stack type piezoactuator.

The quasi-static mechanical response of an open circuit piezoactuator is the one of a mechanical spring. If such an actuator is pulled by an external force *F*, it behaves like a parallel pair of springs with force-displacement law

$$F = (k_p + k_s)x = K_a x \tag{1}$$

where k_p is the mechanical stiffness of the piezoceramic core, k_s is the stiffness of the metallic casing and K_a the combined structural stiffness of the whole actuator.

When the electrodes are connected to an external voltage source u_p, the core is getting a piezoelectric displacement and the actuator force is correspondingly modified to form

$$F = K_a x - k_p d_{33} u_p = K_a x - \alpha u_p \tag{2}$$

where the second term represents the piezoelectric interaction from the electrical system to the mechanical one with the piezoelectric coupling coefficient $\alpha = k_p d_{33}$.

By knowing that the piezoactuator has a capacitance property C_p, an external voltage u_p creates a charge

$$q_p = C_p u_p \tag{3}$$

Moreover, a mechanical extension is generating an additional charge to the piezoelectric core

$$q_p = \alpha x + C_p u_p \tag{4}$$

which is the piezoelectric interaction from the mechanical system to the electrical one (Adriaens 2000, Delibas 2005).

3.1.2 Active damping by classical control rules

Consider now a system given in Figure 5, which has a mass-spring-damper system excited by an external dynamic force f_e and actuated by a piezoelectric stack element, and which at the other end is fixed to the non-moving reference.

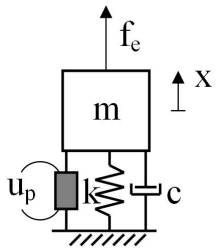

Figure 5. One-degree-of-freedom oscillator connected to a piezoelectric stack actuator.

The equation system governing the oscillatory motion of the mass and fluctuation of the charge in the piezoelement takes the form

$$m\ddot{x} + c\dot{x} + (k + K_a)x = f_e(t) + \alpha u_p \tag{5}$$

$$q_p = \alpha x + C_p u_p \tag{6}$$

This system model is the basis for developing various active damping approaches. The simplest way is to apply one of the known classical control rules. By starting with the principle to utilize the velocity term only, the corresponding rule, which is well known in the classical control theory, is the D-control (Preumont 1997). It compensates the unwanted speed error by the actuator force

$$u_p = K_D(\dot{x}_d - \dot{x}) \tag{7}$$

where K_D is the derivative gain of the controller.

As typical for vibration damping purposes, the desired velocity is set to zero, $\dot{x}_d = 0$, leading to simple so called “direct velocity feedback” rule

$$u_p = -K_D \dot{x} \tag{8}$$

The dynamic equation of the oscillator gets now the form

$$m\ddot{x} + (c + \alpha K_D)\dot{x} + (k + K_a)x = f_e(t) \tag{9}$$

from which one can see, that the velocity feedback is bringing an additional damping to the system, the effect of which can be adjusted by modifying the derivative gain factor. So, the response behaviour is exactly the same as the one of a passively damped oscillator.

By adding to the control rule (7) a position dependent term and requiring also the desired oscillation displacement to be zero, the resulting PD control rule reads

$$u_p = -K_P x - K_D \dot{x} \tag{10}$$

The corresponding dynamic equation of the oscillator is then modified to form

$$m\ddot{x} + (c + \alpha K_D)\dot{x} + (k + K_a + \alpha K_P)x = f_e(t) \tag{11}$$

As compared to the velocity feedback rule, the PD rule is bringing also some additional stiffness to the system (Genta 2009), which can be used for two different purposes:

a) One of the approaches in the classical adaptive control is gain scheduling, which allows one to adaptively modify the gains according to the different system or process states.

b) In the semi-active damping approach one can oscillate or slide the gains in order to modify the damping and the location of the resonance frequency with respect to the excitation frequency.

3.1.3 The use of piezoceramic stack actuator as a shaker

If the external force is replaced by a time-dependent driving voltage u_e, the model actually describes the situation, in which the piezoactuator is used for a shaker purpose (Figure 6).

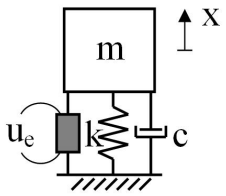

Figure 6. One-degree-of-freedom system under piezoceramic voltage driven shaking load.

The corresponding dynamic equation takes a simple form

$$m\ddot{x} + c\dot{x} + (k + K_a)x = \alpha u_e(t) \tag{12}$$

This is a practical way to make structural and modal testing in cases, where the system parameters of the design are not known.

3.1.4 Piezoelectric damping by using RLC shunt circuit

By adding to the previous model a shunt circuit with resistance, inductance and capacitance connected in series, a tuned passive damper is available (Law 1996).

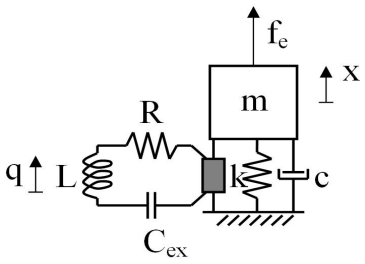

Figure 7. One-degree-of-freedom oscillator connected to a stack actuator and damped by an external serial RLC shunt circuit.

The dynamic equation of motion gets now the form

$$m\ddot{x} + c\dot{x} + (k + K_a)x = f_e(t) + H_p Q \tag{13}$$

where the piezoelectro-mechanical force coefficient is given by

$$H_p = \alpha / C_p \tag{14}$$

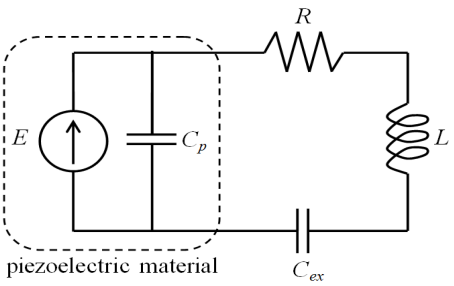

Figure 8. RLC shunt circuit connected to the piezoceramic element with internal capacitance C_p.

By applying the Kirchoff´s loop rule of voltages for a serial connection of a resistance, an inductance and a capacitance, the charge in the shunt circuit is governed by differential equation

$$L\ddot{Q} + R\dot{Q} + \frac{1}{C_{ex}}Q = H_p x \tag{15}$$

The resonance frequency of this circuit is (Moheimani 2006)

$$\omega = \frac{1}{\sqrt{LC_{ex}}} \tag{16}$$

The tuning rule for most of the cases is to choose the circuit parameters L and C_{ex} so that the resonance frequency of the circuit is exactly the same as the lowest eigenfrequency of the structure including the structural stiffness of the piezoactuator.

In comparison to the case of classical controllers, where the motion response can be solved independently from one differential equation of motion, the shunt circuit case requires the simultaneous solution of two differential equations of motion and one differential equation for the electric charge. The coupling structure can be seen even better, when writing the system equations with respect to the state vector

$$\boldsymbol{u} = \begin{Bmatrix} x \\ Q \end{Bmatrix} \tag{16}$$

in form

$$\boldsymbol{M}\ddot{\boldsymbol{u}} + \boldsymbol{C}\dot{\boldsymbol{u}} + \boldsymbol{K}\boldsymbol{u} = f_e(t)\boldsymbol{n} \tag{17}$$

where the combined mass-inductance, damping-resistance and stiffness-capacitance matrices are

$$\boldsymbol{M}=\begin{bmatrix} m & 0 \\ 0 & L \end{bmatrix},\ \boldsymbol{C}=\begin{bmatrix} c & 0 \\ 0 & R \end{bmatrix},\ \boldsymbol{K}=\begin{bmatrix} k+K_a & -H_p \\ -H_p & \dfrac{1}{C_{ex}} \end{bmatrix} \tag{18}$$

with the unit loading vector

$$\boldsymbol{n}=\begin{Bmatrix} 1 \\ 0 \end{Bmatrix} \tag{19}$$

3.2 Response analysis

3.2.1 Analysis methods

Computer analysis of piezoelectric damping systems can be done in time or in frequency domains. Time domain analysis is well argued, if the excitation includes process-specific features. If the response information is stored, a spectrum analysis can be done also later from the interesting quantities. More informative frequency response analysis can be used for evaluation of the resonance risk with respect to periodic known excitations, and for stochastic inputs, whose spectrum is known.

Frequency response analysis in state vector space and in case of RLC shunt circuit has to be done in complex form, because the first order damping-resistance terms make phase shift between the excitation and the response. By writing the excitation in complex form

$$f_e(t)=F_e e^{i\Omega t} \tag{20}$$

the complex amplitude response can be obtained

$$\boldsymbol{U} = F_e\left[-\Omega^2\boldsymbol{M} + i\Omega\boldsymbol{C} + \boldsymbol{K}\right]^{-1}\boldsymbol{n} \tag{21}$$

from which the magnitudes and phase shifts of the displacement oscillation and charge fluctuation can be evaluated.

3.2.2 Evaluation of one-degree-of-freedom responses

The effect of the structural stiffness of the stack actuator has been analyzed by applying the same harmonic excitation to a case study problem without and with the actuator.

The plots of the amplitude at Figure 9 show clearly, that additional stiffness of the piezoactuator together with the stiffening effect of the proportional gain is shifting the resonance frequency from *25.2 Hz* to *51.6 Hz.*

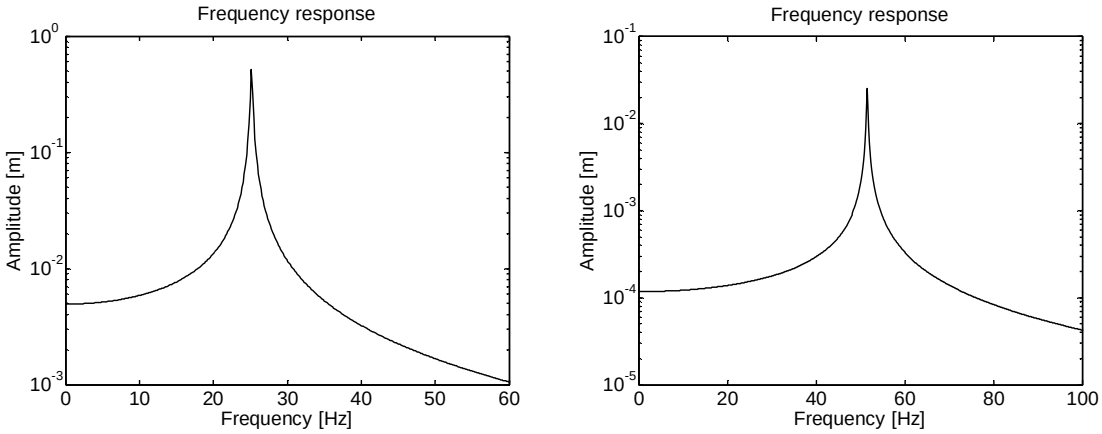

a) b)

Figure 9. Frequency responses of the oscillation amplitude of the one-degree-of-freedom system in two different cases: a) system without the actuator and b) system with the passive actuator.

In the second analysis a serial RLC shunt circuit has been added to damp the motion. A second peak representing the resonance frequency of the shunt circuit is now appearing at higher frequency band in the plot of Figure 10.

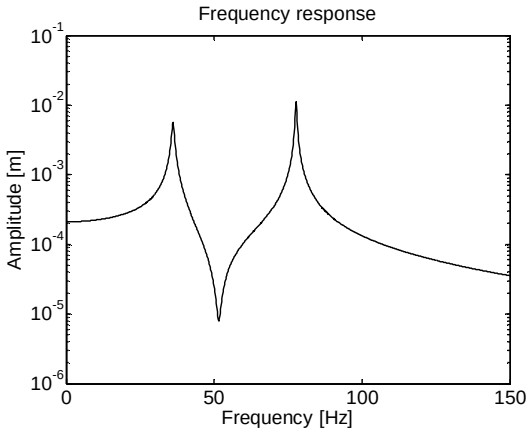

Figure 10. Frequency response of oscillation amplitude under the effect of RLC shunt circuit.

The results of this simple test case show, that the classical controller can be used for moving the resonance far enough from the excitation frequency band, but the performance of shunt circuit is much better at broad frequency band.

4. Piezoelectric damping of rolling contact system

4.1 System description

Expectations to reach higher performance in damping of nip oscillations in paper industry have opened a new research line to use piezoelectric stack actuators in the vibration control of rolling systems. The existing pilot roll press has been completed for that particular research by a pair of piezoceramic stack actuators. A new high precision assembly interface allows stiff mounting of the actuators between the bearing units of the member rolls. The main parts of the nip loading mechanism of the pilot press are shown in Figure 11 and the whole system in Figure 12a.

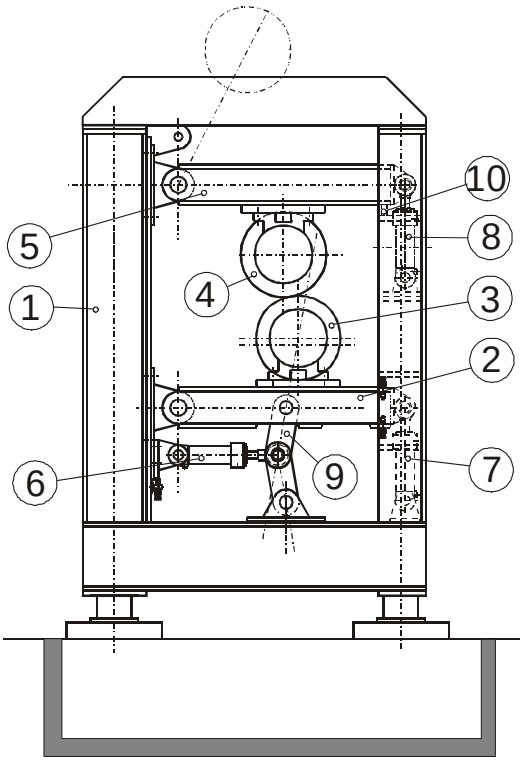

Figure 11. The components and structural parts of the pilot roll press (Kivinen 2001) at the former Laboratory of Machine Dynamics at TUT frame (1), loading arm (2), lower hard roll (3), upper soft roll (4), support arm (5), loading cylinder (6), alternative loading cylinder (7), locking cylinder (8), loading mechanism (9) and load cell (10).

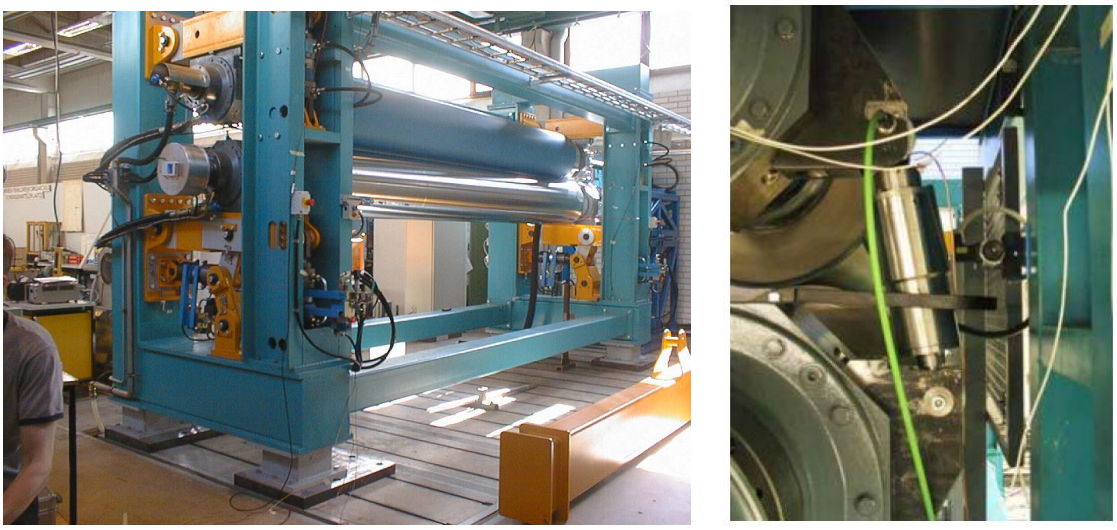

a) b)

Figure 12. Roll loading mechanism at the pilot roll press (a) and the assembly interface of the piezoelectric stack actuators (b). The visible part is the telescopic casing of the linear coupling.

The installation of the piezoactuators between the bearing housings appears in Figure 12b. When closing the roll nip, the lower roll is lifted by the horizontal hydraulic cylinder, which is turning the loading arm by a specific pushing mechanism producing one decade higher nip load than the cylinder itself. To get a correct line load, the nip load is sensed by using a load cell installed between the right end of the support arm of the upper covered roll and the frame. During the nip closing phase, the stack actuators between the roll bearings can slide freely while in the nip closed phase, this linear motion is locked by a stiff fluid powered coupling.

4.2 Plant model of the roll press system

The dynamic plant model consists of sub-system models for rolls, roll covers, roll loading mechanisms, hydraulic actuator circuits and piezoactuators. More detailed structural analysis models are based on distributed parameter models including shell flattening and beam bending effects, but at system level computations over longer process time periods they have to be replaced by simplified mass-spring models.

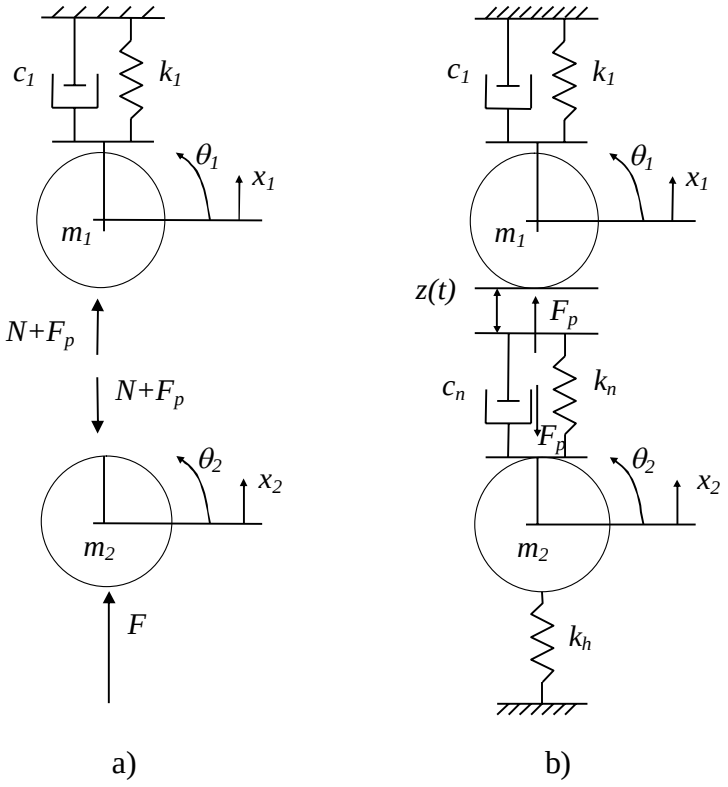

Figure 13. Model of the roll press a) in loading condition and b) in small oscillation situation.

Such two-degree-of-freedom model is illustrated in Figure 13 first in loading condition (a) and in small amplitude oscillation situation (b). A detailed derivation of the dynamic equations of motion of the roll system is given elsewhere (Salmenperä 2013). Due to the nonlinear character of the nip contact, a complete analysis needs simultaneous solution of the static nip deformation equations and the dynamic nip oscillation equations. The nonlinear nip force model

$$N = a\varepsilon^b + c\sqrt{\varepsilon}\dot{\varepsilon} \tag{22}$$

is based on the elastic foundation model (Johnson 1985, Keskinen 2002) of a roll cover made of viscoelastic material following the Kelvin-Voigt material model with elastic modulus E and viscous modulus η .

Model parameters

$$a = \frac{4}{3}\frac{E\ell}{h}\frac{1}{\sqrt{\beta}} \tag{23}$$

$$b = \frac{3}{2} \tag{24}$$

$$c = 2\frac{\eta\ell}{h}\frac{1}{\sqrt{\beta}} \tag{25}$$

$$\beta = ½(R_1^{-1} + R_2^{-1}) \tag{26}$$

depend on the cover thickness h length of the contact line ℓ and on the radii R_1, R_2 of the contacting rolls. Nip compression

$$\varepsilon = x_2 - x_1 + z \tag{27}$$

depends on the relative position between the lower x_2 and upper x_1 rolls and on the thickness variation z of the paper web or the roll cover. It has been shown (Salmenperä 2013) that the dynamic equations of motion governing the small amplitude nip oscillation get form

$$m_1\ddot{x}_1 + (c_1 + c_n)\dot{x}_1 - c_n\dot{x}_2 + (k_1 + k_n)x_1 - k_n x_2 = \gamma k_n (x_1 - x_2)_T - \gamma k_n z_T + c_n\dot{z} + k_n z \tag{28}$$

$$m_2\ddot{x}_2 - c_n\dot{x}_1 + c_n\dot{x}_2 - k_n x_1 + (k_n + k_h)x_2 = \gamma k_n (x_2 - x_1)_T + \gamma k_n z_T - c_n\dot{z} - k_n z \tag{29}$$

The nip stiffness and damping

$$k_n = b\frac{F_d}{\hat{\varepsilon}} \tag{30}$$

$$c_n = c\sqrt{\hat{\varepsilon}} \tag{31}$$

are functions of static nip compression

$$\hat{\varepsilon} = \frac{\left(\frac{F_d}{a}\right)^{1/b}}{1-\gamma} \tag{32}$$

where F_d is the desired nip load and the delay factor of the roll deformation recovery depends on the roll revolution time

$$\gamma = e^{-\frac{E}{\eta}T} \tag{33}$$

Subscript ($_T$) refers to the value of the quantity at the time point roll revolution time T earlier, which is the previous time point when the cover experienced nip compression. For instance $z_T = z(t-T)$. The spring constant of the hydraulic loading mechanism is

$$k_h = B\frac{r^2 A_p}{z_p + r\hat{x}_2} \tag{34}$$

where B is the bulk modulus of oil, r the force magnification factor of the nip loading mechanism, A_p the piston area and z_p the length of the oil chamber.

A typical nip excitation is a sinusoidal thickness variation of the paper web with amplitude Z of form

$$z = Z\sin\Omega t \tag{35}$$

If the web has speed $v = \dot{\theta}_1 R_1$ and wave length λ , this gets expression

$$\Omega = \frac{2\pi\dot{\theta}_1 R_1}{\lambda} \tag{36}$$

The thickness variation has also gradient, which generates a normal velocity

$$\dot{z} = \Omega Z \cos \Omega t \tag{37}$$

4.3 Damping of nip oscillations using classical controllers

When the piezoactuators are connected between the bearing housings, the piezoelectro-mechanical interaction couples the relative roll motion to the charge fluctuation in the piezoelement. The reaction force of the actuator, positive in the pulling direction, is then

$$F_p = K_p(x_1 - x_2) - \alpha u_p \tag{38}$$

The charge in the piezoelement is contributed also by the relative nip motion

$$q_p = \alpha(x_1 - x_2) + C_p u_p \tag{39}$$

In velocity feedback based control the information is taken from the relative roll speed

$$\Delta\dot{x} = \dot{x}_1 - \dot{x}_2 \tag{40}$$

The corresponding D control rule reads

$$u_p = K_D(\Delta\dot{x}_d - \Delta\dot{x}) \tag{41}$$

A relevant principle when limiting nip oscillations, is to require the desired relative speed to vanish, $\Delta\dot{x}_d = 0$, yielding control rule

$$u_p = K_D(\dot{x}_2 - \dot{x}_1) \tag{42}$$

The actuator force then gets the form

$$F_p = K_a(x_1 - x_2) + \alpha K_D(\dot{x}_1 - \dot{x}_2) \tag{43}$$

bringing a contribution to the equations of motion

$$m_1\ddot{x}_1 + (c_1 + c_n + \alpha K_D)\dot{x}_1 - (c_n + \alpha K_D)\dot{x}_2 + (k_1 + k_n + K_a)x_1 - (k_n + K_a)x_2 = \gamma k_n(x_1 - x_2)_T - \gamma k_n z_T + c_n\dot{z} + k_n z \tag{44}$$

$$m_2\ddot{x}_2 - (c_n + \alpha K_D)\dot{x}_1 + (c_n + \alpha K_D)\dot{x}_2 - (k_n + K_a)x_1 + (k_n + k_h + K_a)x_2 = \gamma k_n(x_2 - x_1)_T + \gamma k_n z_T - c_n\dot{z} - k_n z \tag{45}$$

If a more general PD control is used, the control rule reads

$$u_p = K_P(x_2 - x_1) + K_D(\dot{x}_2 - \dot{x}_1) \tag{46}$$

and the actuator force then becomes

$$F_p = (K_a + \alpha K_P)(x_1 - x_2) + \alpha K_D(\dot{x}_1 - \dot{x}_2) \tag{47}$$

The equations of motion are then updated

$$m_1\ddot{x}_1 + (c_1 + c_n + \alpha K_D)\dot{x}_1 - (c_n + \alpha K_D)\dot{x}_2 + (k_1 + k_n + K_a + \alpha K_P)x_1 - (k_n + K_a + \alpha K_P)x_2 = \gamma k_n(x_1 - x_2)_T - \gamma k_n z_T + c_n\dot{z} + k_n z \tag{48}$$

$$m_2\ddot{x}_2 - (c_n + \alpha K_D)\dot{x}_1 + (c_n + \alpha K_D)\dot{x}_2 - (k_n + K_a + \alpha K_P)x_1 + (k_n + k_h + K_a + \alpha K_P)x_2 = \gamma k_n(x_2 - x_1)_T + \gamma k_n z_T - c_n\dot{z} - k_n z \tag{49}$$

By writing this system in vector form

$$\boldsymbol{m}\ddot{\boldsymbol{x}} + \boldsymbol{c}\dot{\boldsymbol{x}} + (\boldsymbol{k} + \boldsymbol{k}_n)\boldsymbol{x} = \gamma \boldsymbol{k}_n \boldsymbol{x}_T + (c_n \dot{z} + k_n z - \gamma k_n z_T)\boldsymbol{n} \tag{50}$$

the terms generated by the piezoactuator can be seen from the system matrices

$$\boldsymbol{m} = \begin{bmatrix} m_1 & 0 \\ 0 & m_2 \end{bmatrix} \tag{51}$$

$$\boldsymbol{k} = \begin{bmatrix} k_1 + K_a + \alpha K_P & -K_a - \alpha K_P \\ -K_a - \alpha K_P & k_h + K_a + \alpha K_P \end{bmatrix} \tag{52}$$

$$\boldsymbol{k}_n = \begin{bmatrix} k_n & -k_n \\ -k_n & k_n \end{bmatrix} \tag{53}$$

$$\boldsymbol{c} = \begin{bmatrix} c_1 + c_n + \alpha K_D & -c_n - \alpha K_D \\ -c_n - \alpha K_D & c_n + \alpha K_D \end{bmatrix} \tag{54}$$

Like in the case of one-degree-of-freedom oscillator, the structural stiffness of the piezoactuator and the control gains can be used to adjust the location of resonance frequencies and the overall damping of the nip oscillation.

4.4 Damping of nip oscillations with passive RLC-circuit

This connection brings again coupled differential equations for the mechanical and electrical sub-systems. The pulling force of the piezoactuator is now

$$F_p = K_a(x_1 - x_2) - H_p Q \tag{55}$$

The voltage output generated by the extensional motion of the piezoelement is

$$u_p = -H_p(x_1 - x_2) \tag{56}$$

By removing the terms related to the PD control and updating the equations with shunt circuit related terms, the equations of motion get form

$$m_1\ddot{x}_1 + (c_1 + c_n)\dot{x}_1 - c_n\dot{x}_2 + (k_1 + k_n + K_a)x_1 - (k_n + K_a)x_2 - H_pQ = \gamma k_n(x_1 - x_2)_T - \gamma k_n z_T + c_n\dot{z} + k_n z \tag{57}$$

$$m_2\ddot{x}_2 - c_n\dot{x}_1 + c_n\dot{x}_2 - (k_n + K_a)x_1 + (k_n + k_h + K_a)x_2 + H_pQ = \gamma k_n(x_2 - x_1)_T + \gamma k_n z_T - c_n\dot{z} - k_n z \tag{58}$$

By adding the voltage output term of the piezoelement, the charge equation reads

$$L\ddot{Q} + R\dot{Q} + \frac{1}{C}Q - H_p x_1 + H_p x_2 = 0 \tag{59}$$

For getting better insight to the coupling structure, the equations are written in state vector form

$$\boldsymbol{M}\ddot{\boldsymbol{y}} + \boldsymbol{C}\dot{\boldsymbol{y}} + \boldsymbol{K}\boldsymbol{y} + \boldsymbol{K}_n\boldsymbol{y} = \gamma\boldsymbol{K}_n\boldsymbol{y}_T + (c_n\dot{z} + k_n z - \gamma k_n z_T)\boldsymbol{N} \tag{60}$$

where the state and the unit load vectors are

$$\boldsymbol{y} = \begin{Bmatrix} x_1 \\ x_2 \\ Q \end{Bmatrix} \tag{61}$$

$$\boldsymbol{N} = \begin{Bmatrix} 1 \\ -1 \\ 0 \end{Bmatrix} \tag{62}$$

The system matrices are

$$\boldsymbol{M} = \begin{bmatrix} m_1 & 0 & 0 \\ 0 & m_2 & 0 \\ 0 & 0 & L \end{bmatrix} \tag{63}$$

$$\boldsymbol{C} = \begin{bmatrix} c_1 + c_n & -c_n & 0 \\ -c_n & c_n & 0 \\ 0 & 0 & R \end{bmatrix} \tag{64}$$

$$\boldsymbol{K} = \begin{bmatrix} k_1 + K_a & -K_a & -H_p \\ -K_a & k_h + K_a & H_p \\ -H_p & H_p & C_{ex}^{-1} \end{bmatrix} \tag{65}$$

$$\boldsymbol{K}_n = \begin{bmatrix} k_n & -k_n & 0 \\ -k_n & k_n & 0 \\ 0 & 0 & 0 \end{bmatrix} \tag{66}$$

For tuning the eigenfrequency of the shunt circuit, one has to determine the structural eigenfrequencies of the two roll system. In the particular case, when the rolls have an equal mass, the non-damped natural frequencies can be computed from the expression

$$\omega^2 = \frac{1}{2M}\left[K_1 + K_2 \pm \sqrt{(K_1 - K_2)^2 + 4K^2} \right] \tag{67}$$

in which the following notations have been used

$$M = m_1 = m_2 \tag{68}$$

$$K = k_n + K_a \tag{69}$$

$$K_1 = k_1 + K \tag{70}$$

$$K_1 = k_h + K \tag{71}$$

From the two vibration modes, the lower one represents synchronous motion of the rolls, while the higher one is related to the non-synchronous roll-against-roll mode. This mode is relevant in the nip oscillation case and the RLC circuit should be tuned close enough to the corresponding frequency.

5. Computer simulation of rolling contact with piezoelectric damping

5.1 Numerical solution of state equations in time and frequency domains

State equations of rolling contact systems with polymer covers are delay differential equations. In time domain analysis the computational platform must provide directly, or allow the user to program codes, for handling the delayed information. If such subroutines or functions are available, the differential equation system can be integrated in the time domain like any problem including nonlinearities.

The frequency response analysis differs also from the one of regular differential systems. By writing the harmonic thickness variation in the complex form

$$z(t) = Ze^{i\Omega t} \tag{72}$$

and by recalling the definition (33) of delay factor γ, the complex amplitude response of the delay systems (50) or (60) can be solved

$$\boldsymbol{X} = Z\left(i\Omega c_n + \chi(\Omega)k_n\right)\left[-\Omega^2\boldsymbol{m} + i\Omega\boldsymbol{c} + \boldsymbol{k} + \chi(\Omega)\boldsymbol{k}_n\right]^{-1}\boldsymbol{n} \tag{73}$$

in which the delay effect is controlled by the complex expression

$$\chi(\Omega) = 1 - e^{-\frac{T}{\tau_r}}e^{-i2\pi\frac{T}{T_e}} \tag{74}$$

with the polymer relaxation time $\tau_r = \eta/E$ and the duration time T_e of one excitation oscillation.

If the ratio T/T_e gets an integer value

$$T = nT_e \tag{75}$$

factor (74) becomes real

$$\chi(\Omega) = 1 - e^{-\frac{T}{\tau_r}} \tag{76}$$

and in this particular case, the shorter the rotation time is, the smaller is the effective nip stiffness due to the small values of this reduction factor, and in order to avoid instabilities the system needs artificial damping and stiffness by means of an additional actuator system.

Figures 14a and 14b show the frequency responses of the original system without an additional damper. From the plots one can identify the wide resonance peak clusters, which are arising from the delay effect in the system.

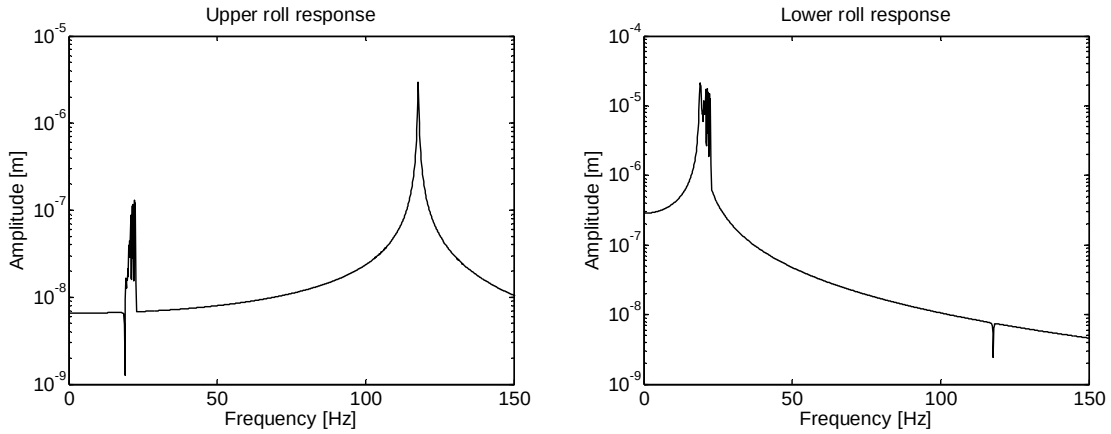

a) b)

Figure 14. Frequency response of a) upper and b) lower roll without the additional damper.

5.2 Response of roll press damped with classical control rules

Frequency and time domain plots of roll motions with D control based active vibration damper are presented below in Figures 15 and 16. Results show that the additional vibration damping system increases the stiffness of the system and brings damping to stabilize it.

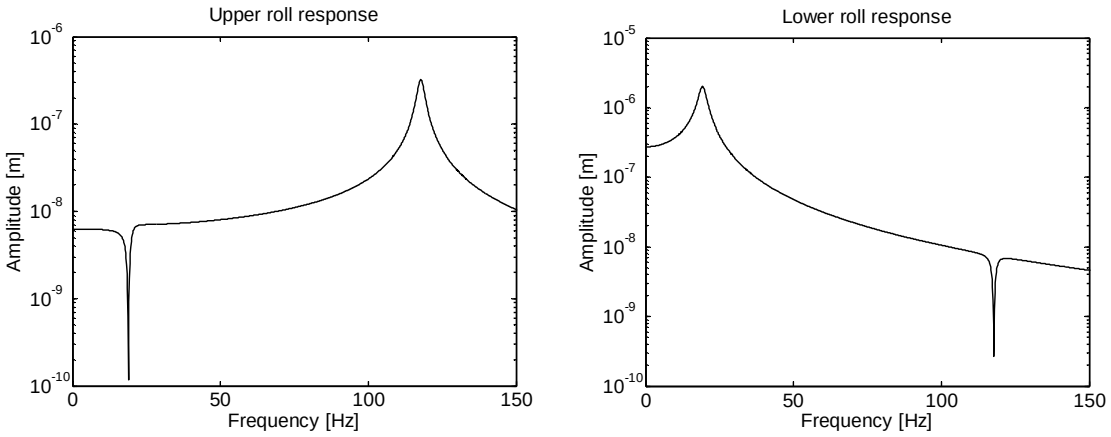

a) b)

Figure 15. Frequency responses of upper (a) and lower roll (b) displacements with D control.

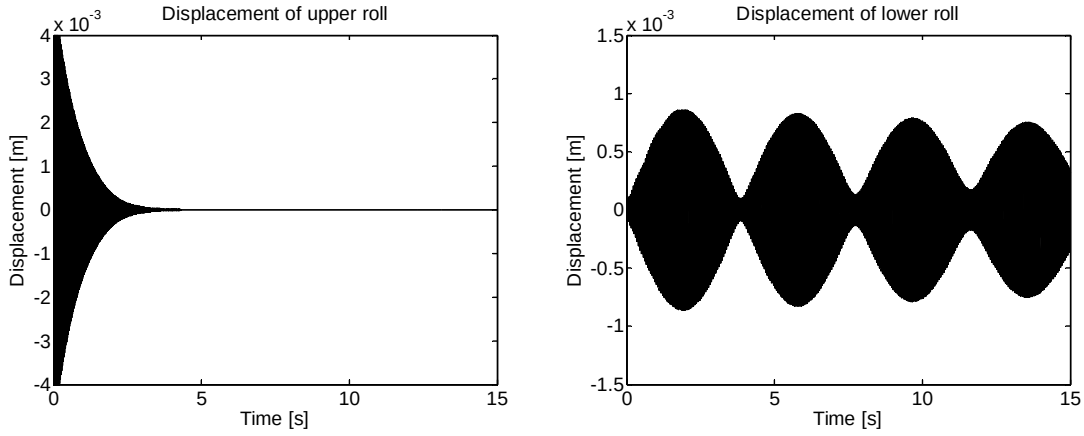

a) b)

Figure 16. Transient responses of a) upper and b) lower roll displacements with D control.

The control voltages and force produced by the piezoactuator during and after transient activation of the damper appear in Figures 17a and 17b. The limit-cycle oscillation of the actuator force stays below the maximum capacity the piezoelement can produce.

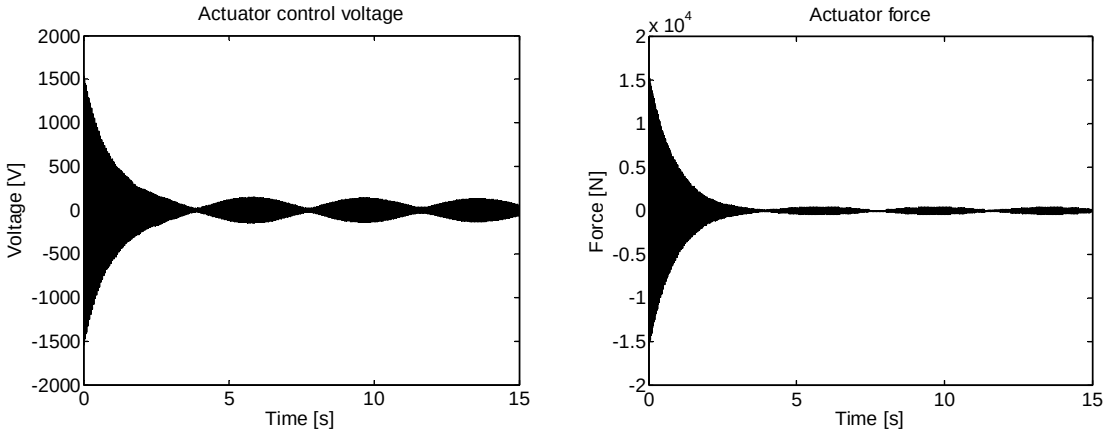

a) b)

Figure 17. Transient responses of control voltage (a) and actuator force (b) with D control.

Frequency response plots of roll press system with active vibration damper by means of a classical PD controller are presented below in Figures 18a and 18b.

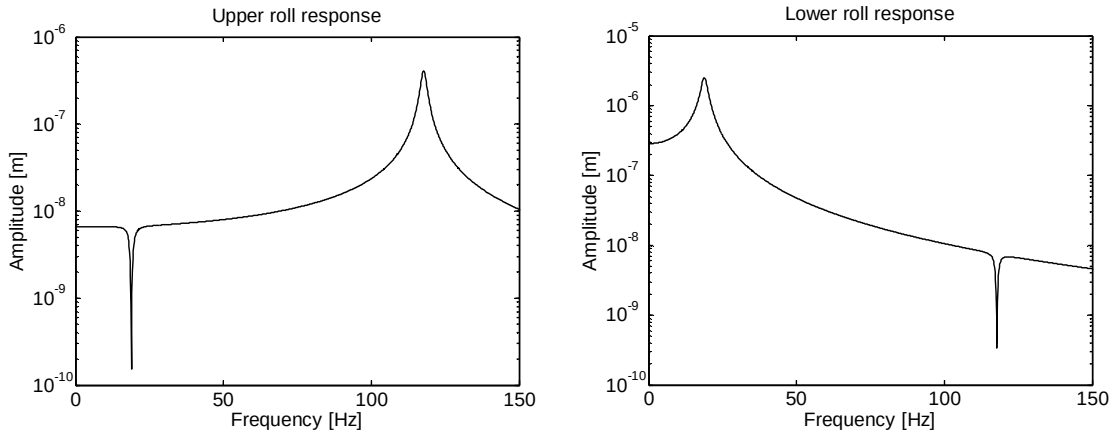

a) b)

Figure 18. Frequency responses of upper (a) and lower roll (b) displacements with PD control.

The stiffness effect of proportional gain is shifting the second resonance to a higher frequency. The initial out-of-equilibrium transient motion of rolls (Figure 19) is stabilized effectively and the small radius of the limit-cycle oscillation after the attenuation phase shows excellent damping performance. Similar behaviour can be observed in the circuit response keeping the final voltage and actuator force fluctuations (Figure 20) in acceptable bounds as well.

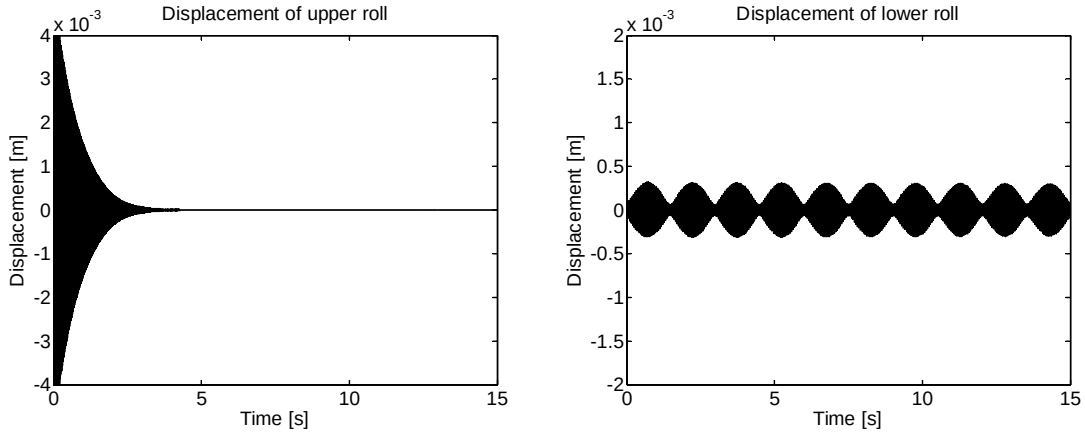

a) b)

Figure 19. Time histories of a) upper and b) lower roll motions with PD control.

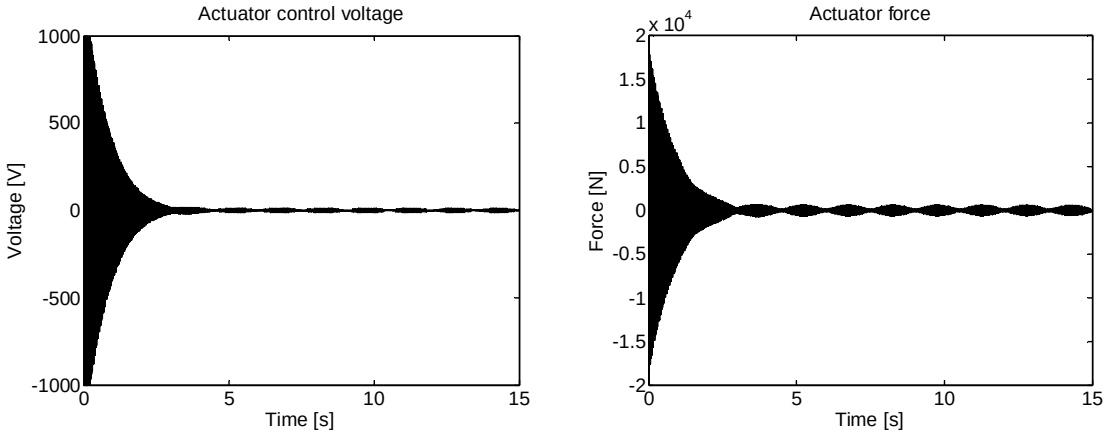

a) b)

Figure 20. Transient responses of control voltage (a) and actuator force (b) with PD control.

5.3 System response using passive RLC-circuit

Frequency and time domain plots of roll motions with passive shunt damper are presented below in Figures 21 and 22. The damping circuit components were tuned to produce the first natural frequency at *19.33 Hz*. At this frequency the damping performance is excellent. This was achieved with inductance $L = 25.12\ H$, resistance $R = 200\ \Omega$ and capacitance $C = 2.7\ \mu F$.

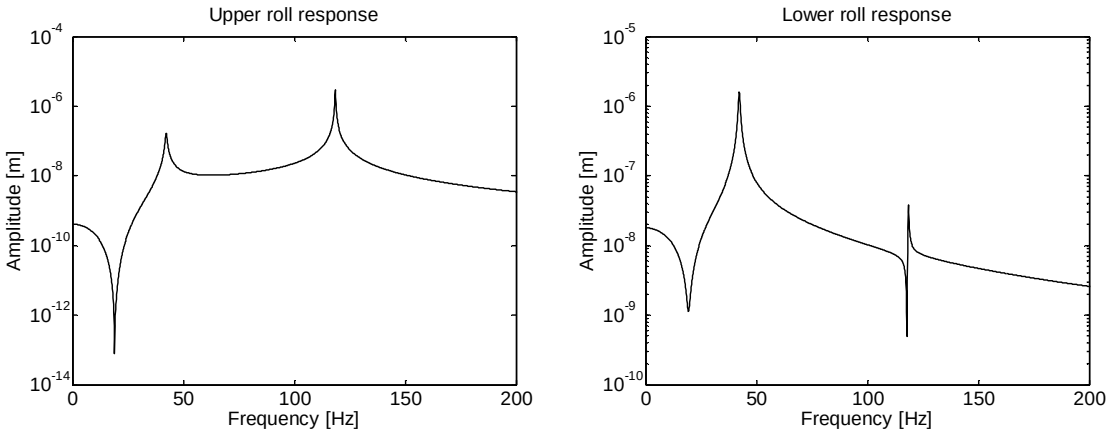

a) b)

Figure 21. Frequency responses of upper (a) and lower roll (b) motions with RLC shunt circuit tuned to the first natural frequency.

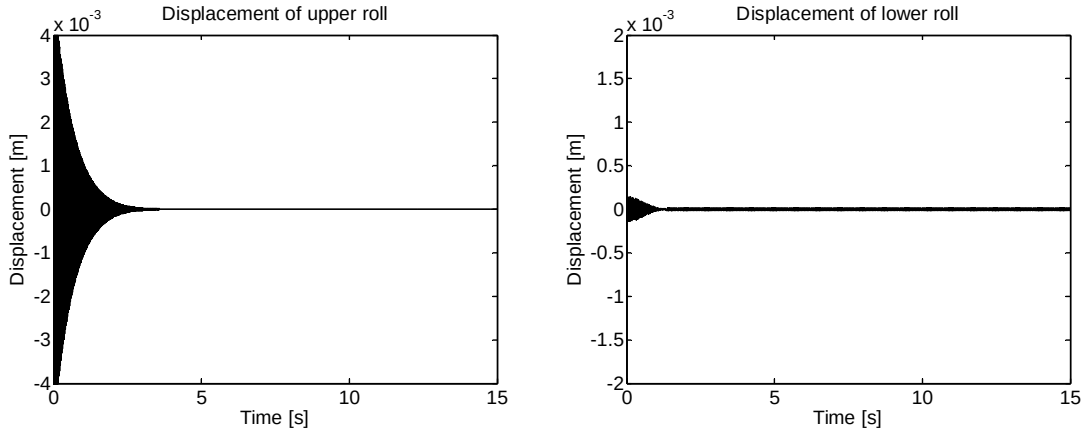

a) b)

Figure 22. Time histories of a) upper and b) lower roll motions with RLC shunt circuit tuned to the first natural frequency.

The electric charge in RLC circuit is plotted in Figure 23a. Also the total voltage over RLC circuit remains under the maximum applicable voltage of the actuator as shown in Figure 23b.

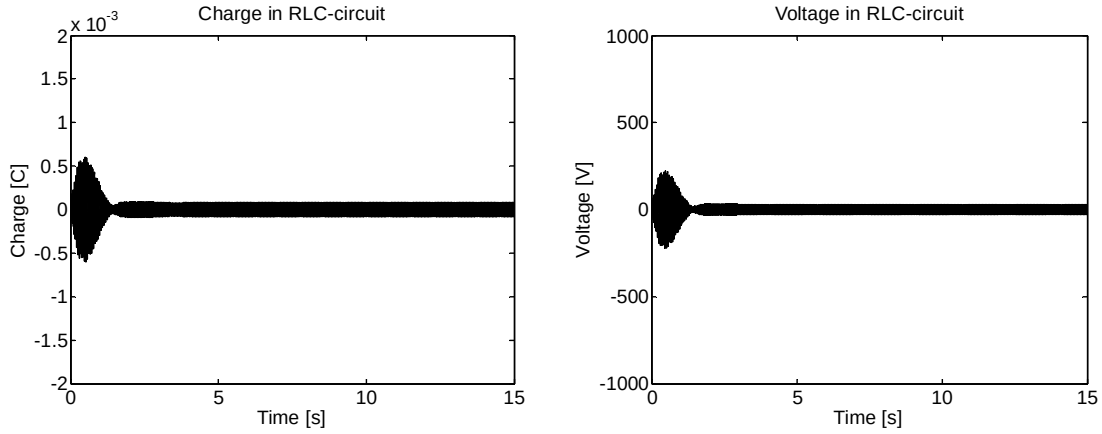

a) b)

Figure 23. Electric charge in the circuit (a) and voltage over the actuator electrodes (b) when tuned to the first natural frequency.

The damping circuit components may also be tuned to the second natural frequency at *117.8 Hz*, at which the unwanted nip vibration in roll-against-roll mode takes place. Frequency and time domain plots of roll motions are presented below in Figures 24 and 25. At this frequency the damping performance is excellent. This was achieved with inductance $L = 0.27\ H$, resistance $R = 200\ \Omega$ and capacitance $C = 10.8\ \mu F$.

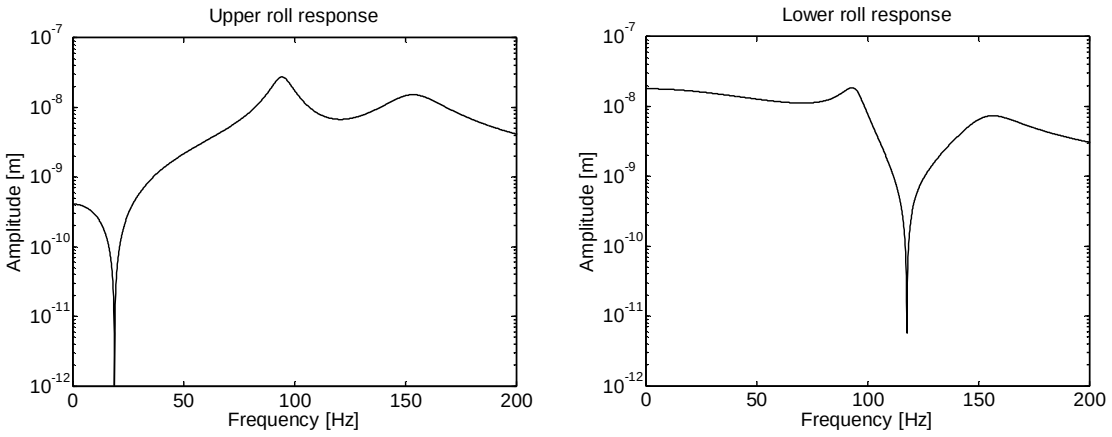

a) b)

Figure 24. Frequency responses of upper (a) and lower roll (b) motions with RLC shunt circuit tuned to the second natural frequency.

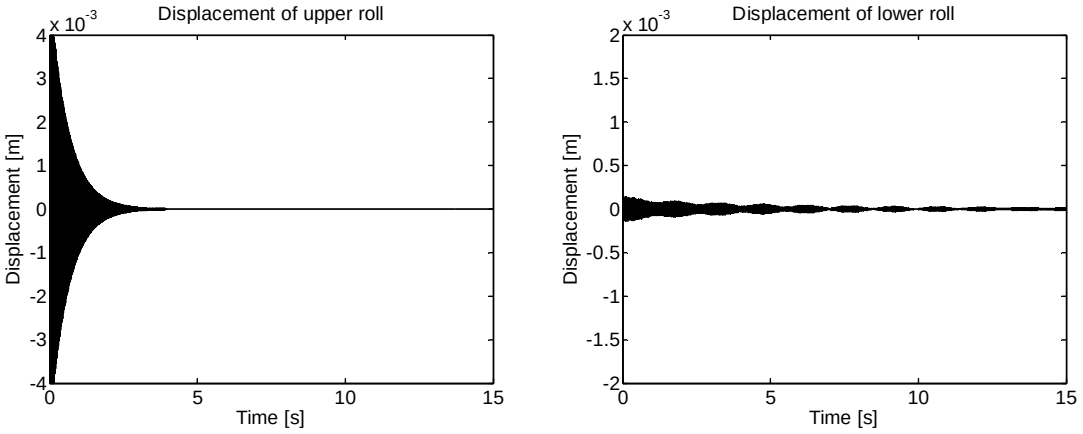

a) b)

Figure 25. Time histories of a) upper and b) lower roll motions with RLC shunt circuit tuned to the second natural frequency.

The electric charge in RLC circuit is plotted in Figure 26a. Also the total voltage over RLC circuit remains under the maximum applicable voltage of the actuator as shown in Figure 26b.

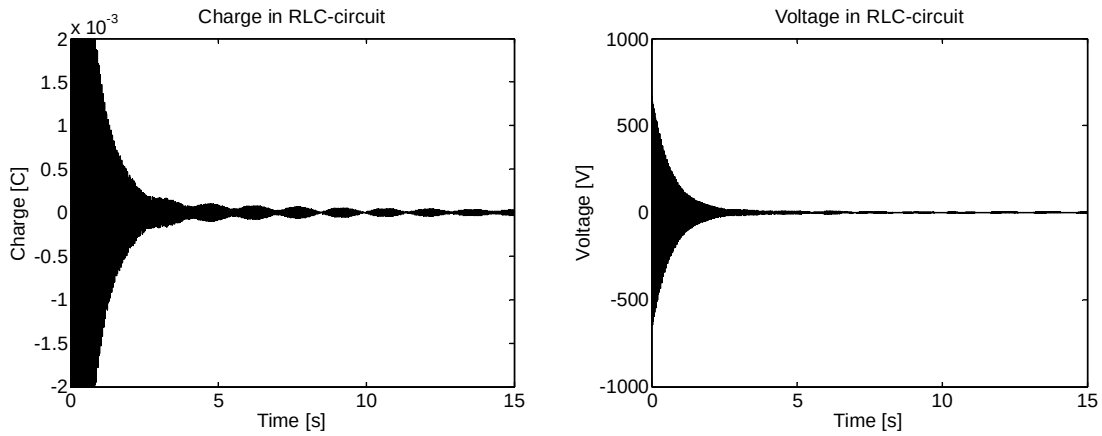

a) b)

Figure 26. Electric charge in the circuit (a) and voltage over the actuator electrodes (b) when tuned to the second natural frequency.

6. Experimental testing of piezoelectric damping system

A realization of the piezoelectric damping system for a rolling contact system has been implemented in an existing pilot roll press. This system consists of two similar actuators, one for each end of the roll stack, of two voltage sources with related amplification electronics and a signal generator. The actuators are inside of a linear coupling making it possible to activate or deactivate the actuators during nip closing or opening operations. A set of separate tests have been carried out to identify the characteristic properties of the actuator set-up. This includes the evaluation of the force and motion output of the actuators, modal analysis of the roll stack with and without the actuators and finally the frequency response analysis of the roll stack for shaking excitation driven by the piezoactuators.

6.1 Characterization of piezoelectric actuator in force and motion control

In order to find out the characteristics of a piezoelectric actuator the free elongation or the stroke and the force generation of the actuator may be measured. The measurement arrangement is shown in Figure 27a. Two different control signal frequencies of *60 Hz* and *125 Hz* were used.

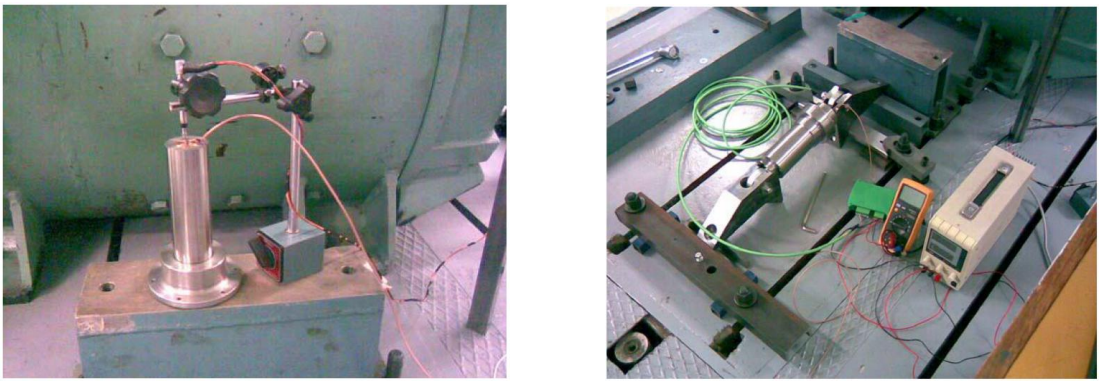

a) b)

Figure 27. Measurement set-up to identify actuator motion (a) and force (b) characteristics.

The displacement results are shown in Figure 28. As mentioned earlier the nominal stroke provided by the manufacturer for the piezoelectric actuator used in experiments is *60 μm*. The displacement was obtained by integrating the acceleration signal measured with B&K 4375 sensor and B&K 2635 amplifier. The voltage source was adjusted so that the piezoactuator maximum nominal voltage of *1000 V* is achieved, which corresponds to the output monitoring voltage *10 V*. Results show that the nominal stroke of *60 μm* is achieved already with approximately *450 V*, corresponding to the monitoring voltage *4.5 V*. Also the hysteresis effect of the piezoelectric actuator is clearly visible.

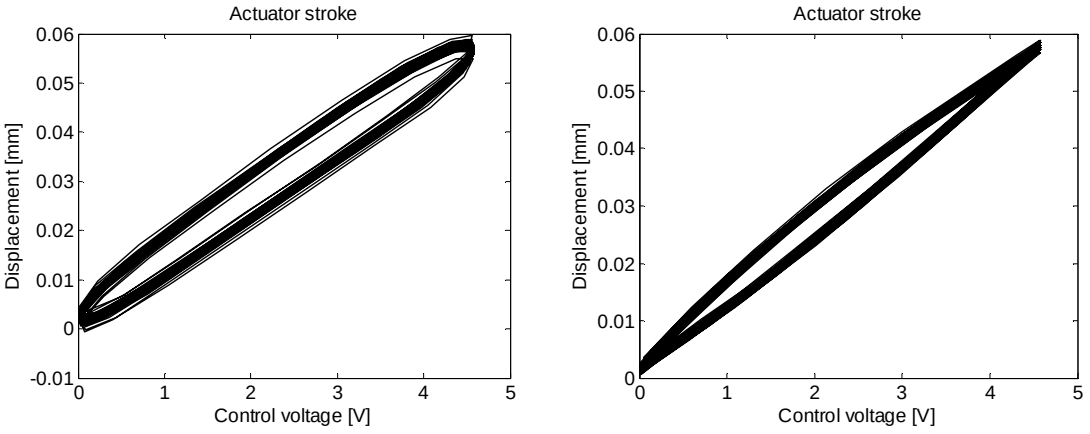

a) b)

Figure 28. Piezoelectric actuator strokes with 60 Hz and 125 Hz driving frequency.

The force generation of the piezoelectric actuator was measured with control signal frequency of *125 Hz* for two different amplitudes, *1.2 V* and *1.4 V*. The measurement arrangement is shown in Figure 27b. The actuator force was measured with a pin type force sensor, which is based on strain gage information. Sensor was placed in a lug attached to the actuator. The actuator was placed inside the casing, in which it will be installed into the pilot roll press. The voltage source was adjusted so that the maximum control voltage of *1000 V* is achieved giving output monitoring voltage of *10 V*. The preload compression of *0.6 kN* for the actuator was set to eliminate all gaps in test set-up. The measurement results are shown in Figures 29a and 29b. One problem related to piezoelectric actuators, which rose up in measurements, is the

flexibility of the supporting structure and attachments. As seen from the force – voltage curves the major part of the actuator stroke is lost in structural deformation. The nominal maximum force provided by the manufacturer for the piezoelectric actuator used in experiments is *12 kN* whereas the measured force value is limited to approximately *0.6 kN*. This indicates that the piezoelectric actuator reaches its maximum stroke and is not able to generate more force. The flexibility of the support structure can also be seen from the nonlinear shapes of the force - voltage hysteresis loops.

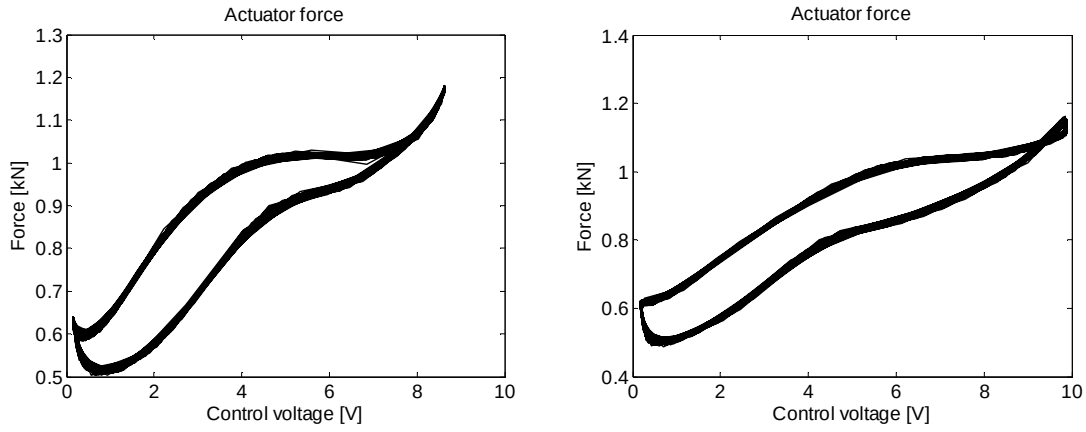

a) b)

Figure 29. Piezoelectric actuator force with amplitudes a) *1.2 V* (*= 857 V*) and b) *1.4 V* (*=1000 V*).

6.2 Modal analysis of the roll press with piezoelectric damper

The influence of the dampers on the stiffness of the supporting structure of the rolls was studied by measuring the frequency response (FRF) of the system. The measurements were carried out by hammer tests with the piezoactuated dampers installed into the pilot roll press. In measurements the piezoelectric actuator stack was first free and then pre-loaded by *1 kN* compressive force and simultaneously a *400 V* signal was fed into the actuators to generate the additional stiffness of the working piezoactuator vibration damper. The compressive line load between rolls was set to *15*

kN/m and rolls were not rotating. Responses were measured from the bearing housings and from the middle of both rolls. The locations of the excitation and the response points are listed in Table 1.

Table 1. Measurement points in modal testing.

Point number	**Point location** TE = tender end; DE = drive end
1	TE lower roll casing end, hammer hit excitation
2	TE lower roll bearing housing
3	TE upper roll bearing housing
4	DE lower roll bearing housing
5	DE upper roll bearing housing
6	Lower roll centre
7	Upper roll centre

In results the FRF graphs of each response point are shown. The measured parameter is mobility (velocity/force) in unit $ms^{-1}N^{-1}$. The measurement equipment was the LMS Scads III with Test.Lab software and transducers were ICP type Kistler accelerometers and force transducer. The results without the additional stiffness of the actuators are shown in Figures 30a, 31a, 32a, 33a, 34a, 35a and results with the additional stiffness of the actuators in Figures 30b, 31b, 32b, 33b, 34b, 35b. Summary of the modal frequencies and damping values are tabulated in Table 2. Results show that installation of the piezoactuated vibration damper does not have significant influence on the modal parameters of the pilot roll press.

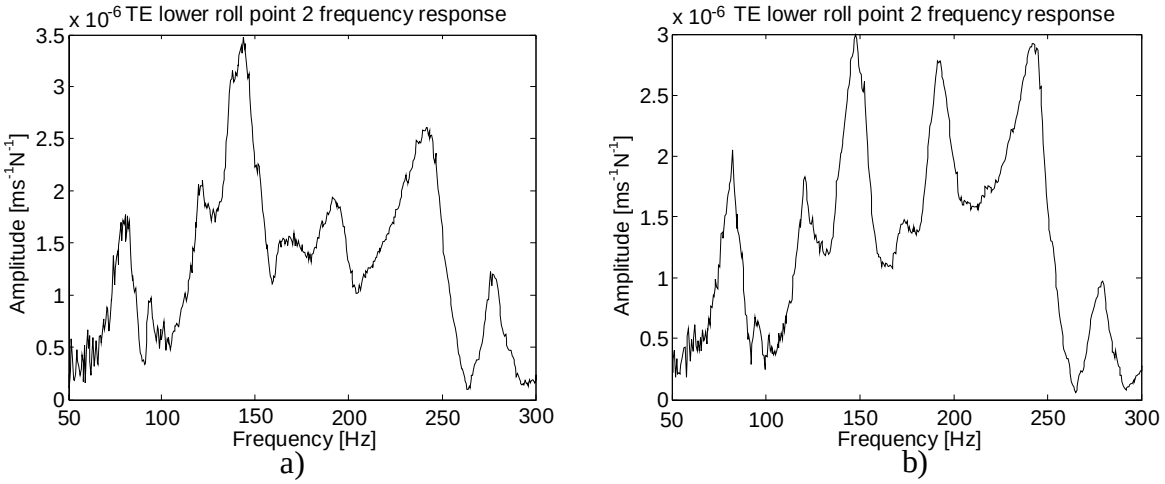

Figure 30. Mobility of point 2 at TE lower roll bearing housing a) without and b) with the damper.

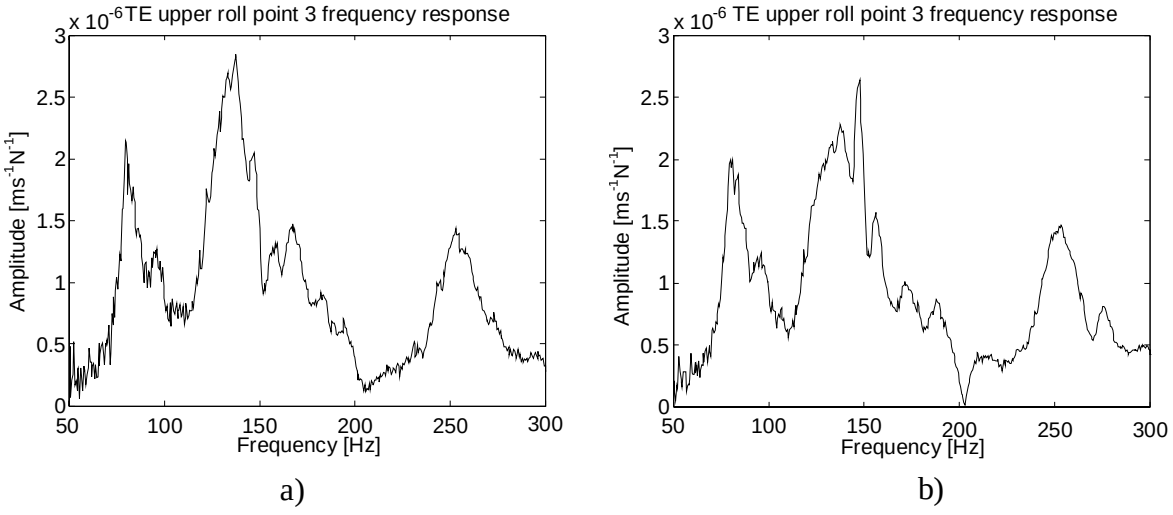

Figure 31. Mobility of point 3 at TE upper roll bearing housing a) without and b) with the damper.

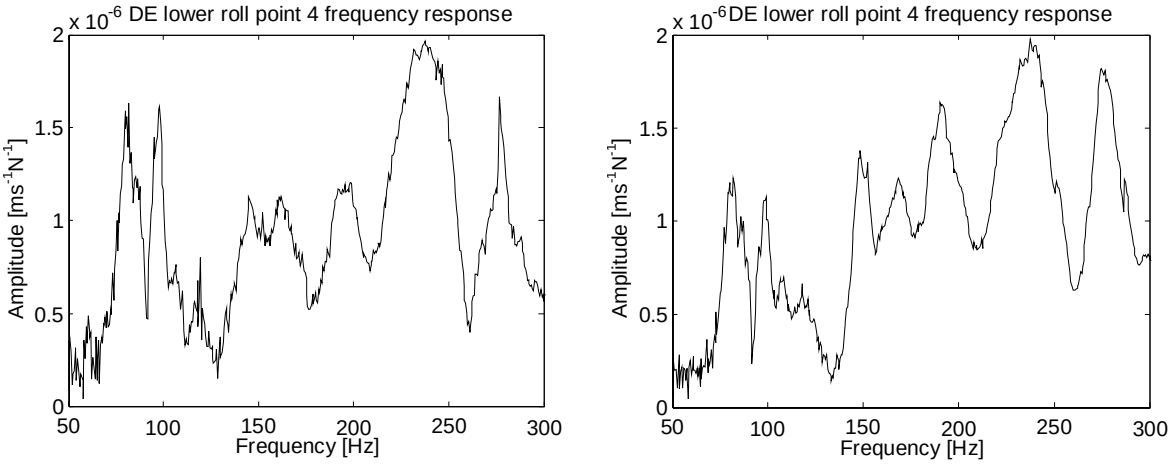

Figure 32. Mobility of point 4 at DE lower roll bearing housing a) without and b) with the damper.

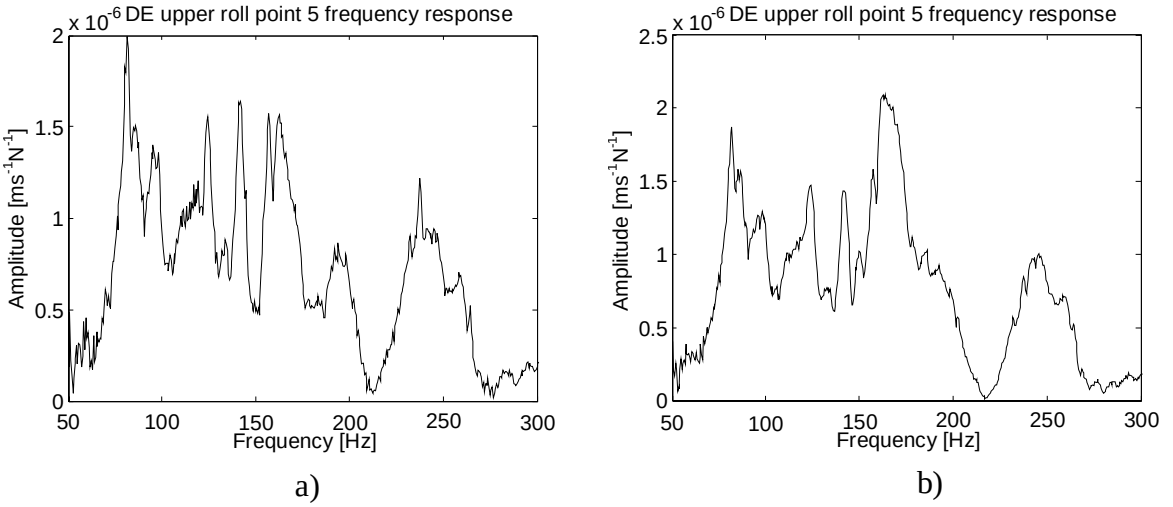

Figure 33. Mobility of point 5 at DE upper roll bearing housing a) without and b) with the damper.

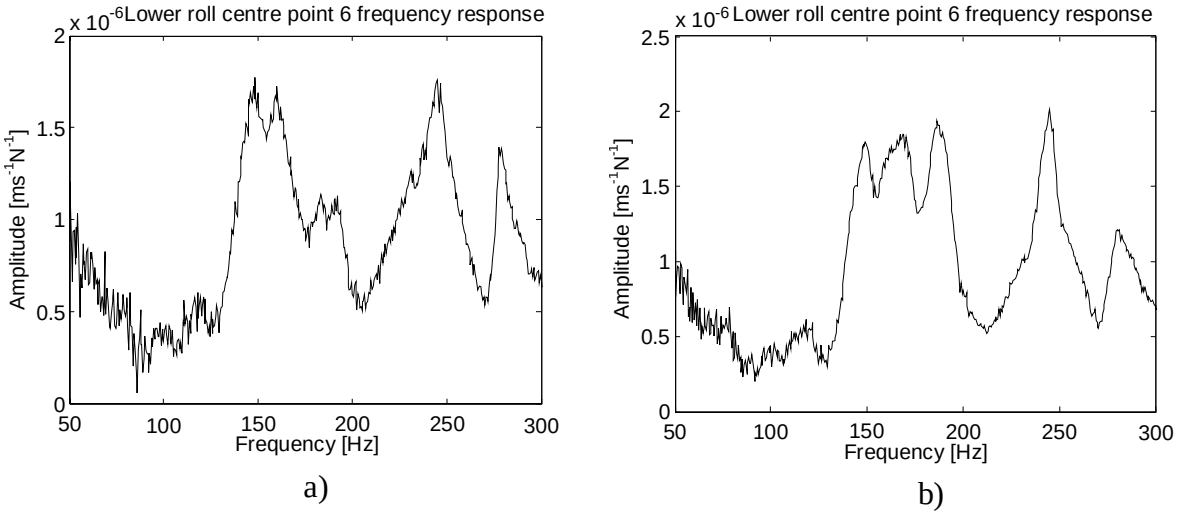

Figure 34. Mobility of point 6 at lower roll centre a) without and b) with the damper.

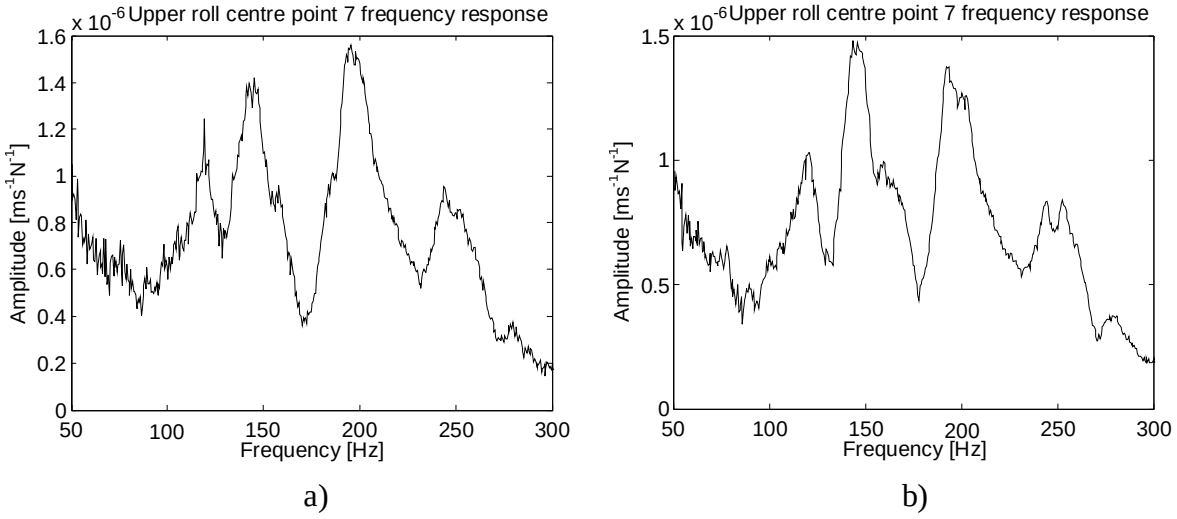

Figure 35. Mobility of point 7 at upper roll centre a) without and b) with the damper.

Table 2. Modal parameter comparison without and with additional stiffness of the damper.

Without damper stiffness		**With damper stiffness**	
Frequency (*Hz*)	Damping (*%*)	Frequency (*Hz*)	Damping (*%*)
35.4	*1.9*	*35.9*	*2.7*
81.1	*4.9*	*81.8*	*5.0*
95.6	*0.9*	*96.5*	*0.8*
122.9	*3.2*	*122.4*	*4.3*
140.2	*3.7*	*145.5*	*2.9*
163.4	*2.3*	*168.1*	*2.3*

(Barring frequency is approximately *122 Hz*)

6.3 Response of roll press to shaking input driven by piezoactuators

After installing the piezoelectric vibration dampers the vibration response of the pilot roll press was studied also with peak hold spectrum and water fall spectrum measurements. In measurements both piezoelectric actuators were used as shakers and they were controlled by a signal generator. Peak hold spectra were measured in band width (piezoelectric actuator vibration frequency) of 80 *Hz – 300 Hz*, with *444 V* of actuator driving voltage and control signal amplitude of *0.3 V* and actuator pre-load of *1 kN*. Rolls rotational frequency was *0.5 Hz*. Water fall spectra was measured in band width of *100 Hz – 150 Hz*, with *500 V* of actuator driving voltage and control signal amplitude *0.5 V* and actuator pre load of *1 kN*. Roll rotational frequency was *4 Hz*.

Peak hold measurement results are shown in Figure 36. The following resonance frequencies can be identified from the measurements: *86 Hz, 100 Hz, 124 Hz, 167 Hz, 186 Hz 194 Hz, 223 Hz, 274 Hz.*

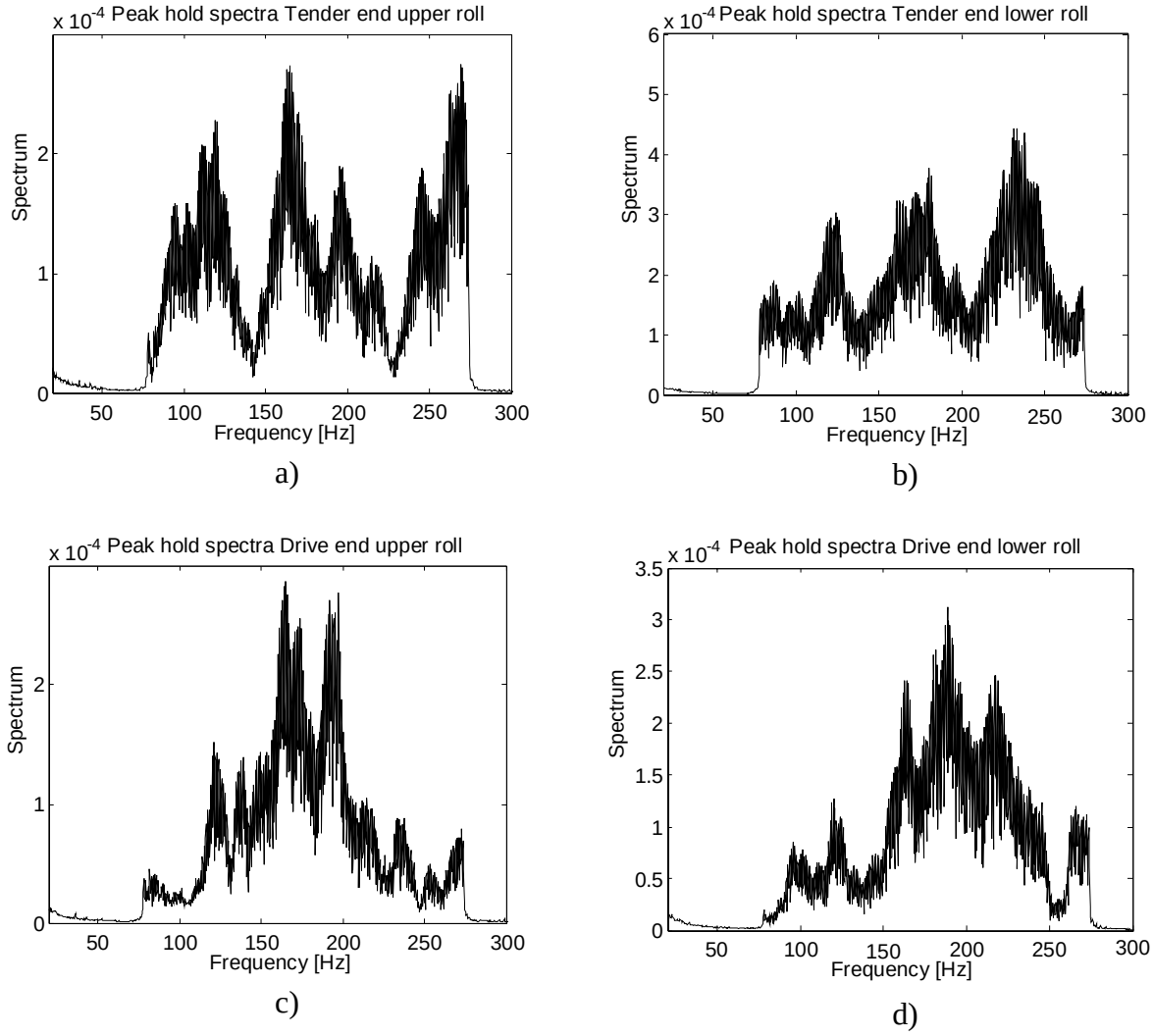

Figure 36. Peak hold displacement spectra of a) TE upper roll, b) TE lower roll, c) DE upper roll and d) DE lower roll.

Water fall measurement results are shown in Figures 37 and 38. In water fall representation the barring frequency and some other resonance frequencies can be identified as well.

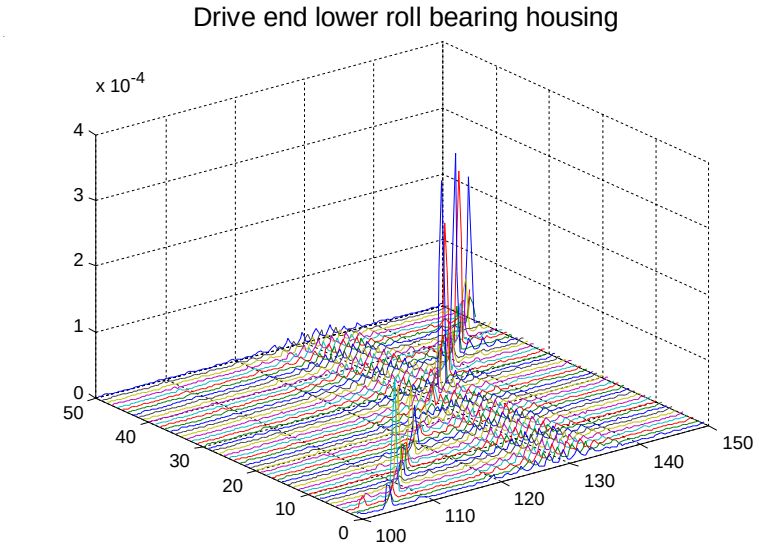

a)

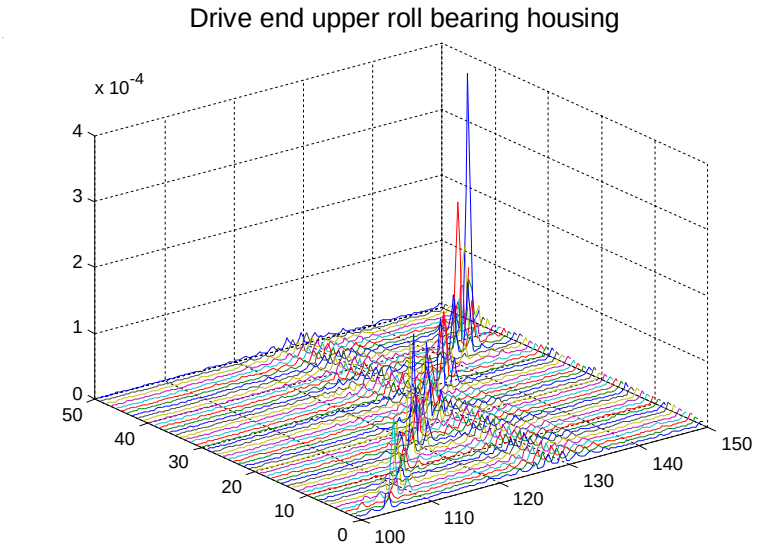

b)

Figure 37. Waterfall spectra of bearing housing displacements at drive end in frequency band *100-150 Hz* for a record of *50 s*.

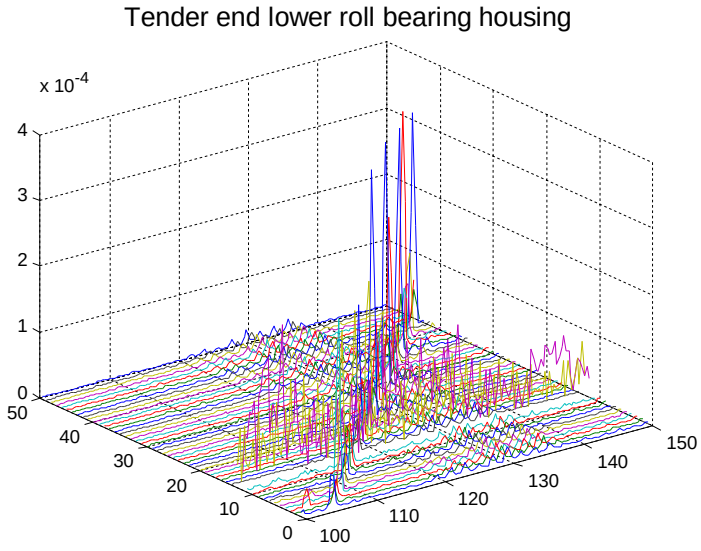

a)

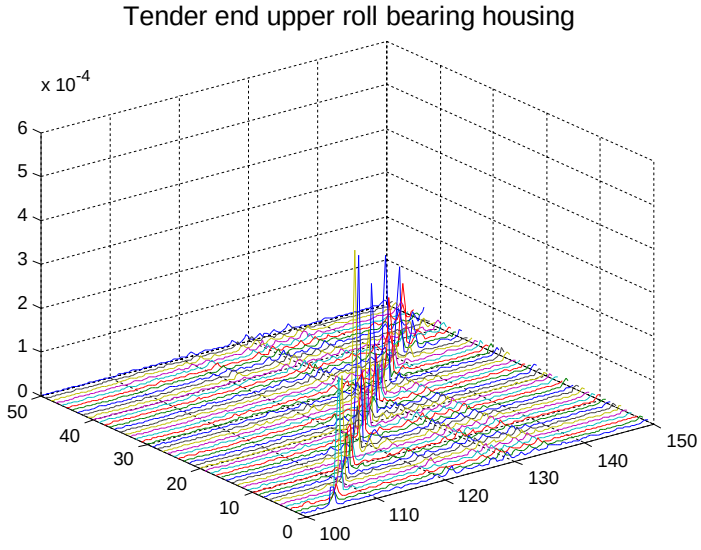

b)

Figure 38. Waterfall spectra of bearing housing displacements at tender end in frequency band *100-150 Hz* for a record of *50 s*.

7. Performance analysis of piezoelectric actuators in damping of nip vibration

A set of particular test cases have been carried out to evaluate the performance of the piezoelectric vibration damping circuit. In the first test case the damping circuit is open, in which situation the actuator is passively restricting the relative motion between the roll bearing housings by the structural stiffness of the piezoactuator itself. In the second case the damping circuit is active, bringing the contribution of the derivative gain in the D control (direct velocity feedback) scheme. In the third and fourth cases the point and cross receptances of the roll ends were evaluated by using the piezoactuators simultaneously in shaker and damper modes.

7.1 Response to geometric errors in the case of damping circuit open

After mounting the vibration damper between bearing housings the dead load of the piezoelectric actuators arising from manufacturing and installation errors of the pilot roll press was investigated. The actuator force was measured with load sensors in series with actuators. The rotational frequency of rolls was *0.5 Hz* in all measurements.

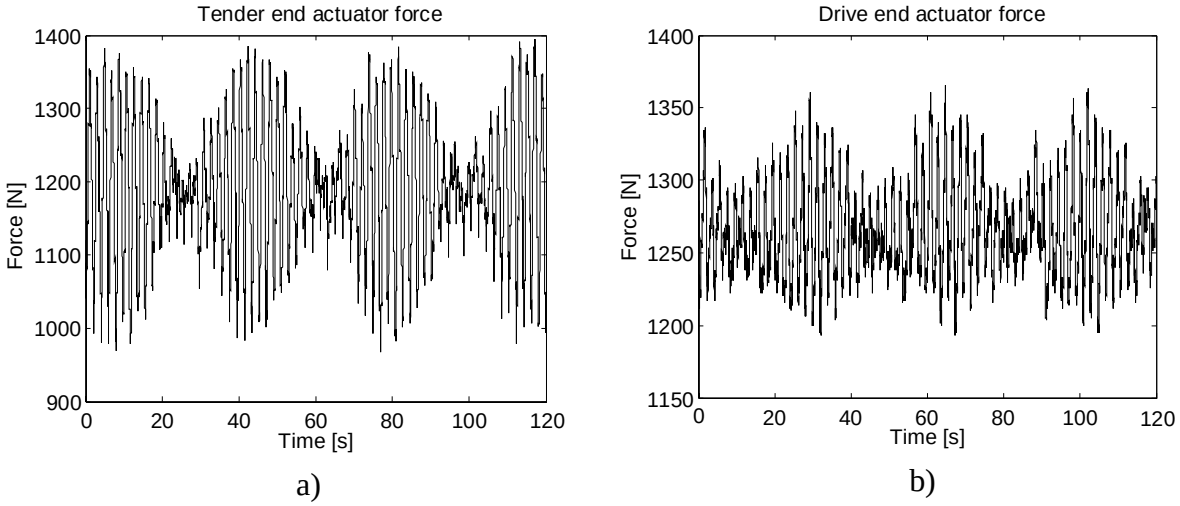

a) b)

Figure 39. TE actuator force (a) and DE actuator force (b).

In Figure 39 the force variation of both ends is shown. The static preload of actuator was set to approximately *1.17 kN*. The force variation originates mainly from the eccentricities of the rolls. Maximum peak-to-peak force in TE damper was *0.4 kN*.

7.2 Response to varying excitation amplitude in the case of damping circuit closed

The actuator force generation and relative motion of bearing housings in both ends was studied for different excitation frequencies and constant amplitudes of the piezoelectric actuator. In measurements the rotational frequency was set again to *0.5 Hz*, actuator driving voltage to *444 V* and control signal amplitude variation in the range from *0.3* to *1.0 V* while excitation frequency was set to a fixed value of *80 Hz*. Displacement was measured with LVDT sensor and the actuators were following an artificially generated shaking signal in a position control servo loop.

In Figure 40 the force generation of tender end piezoelectric actuator is shown. The maximum peak-to-peak force is *1.3 kN*. When the force measured without actuator control is subtracted, the net force produced by the actuator is about *0.9 kN*. The maximum peak-to-peak displacement is *0.02 mm*. When the compression by preload is subtracted, the net displacement generated by the actuator is *0.01 mm* (maximum stroke of the actuator is *0.06 mm*). In Figure 40c is shown the displacement of the lower TE bearing housing measured with the accelerometer. The maximum amplitude (absolute) is *0.0025 mm*.

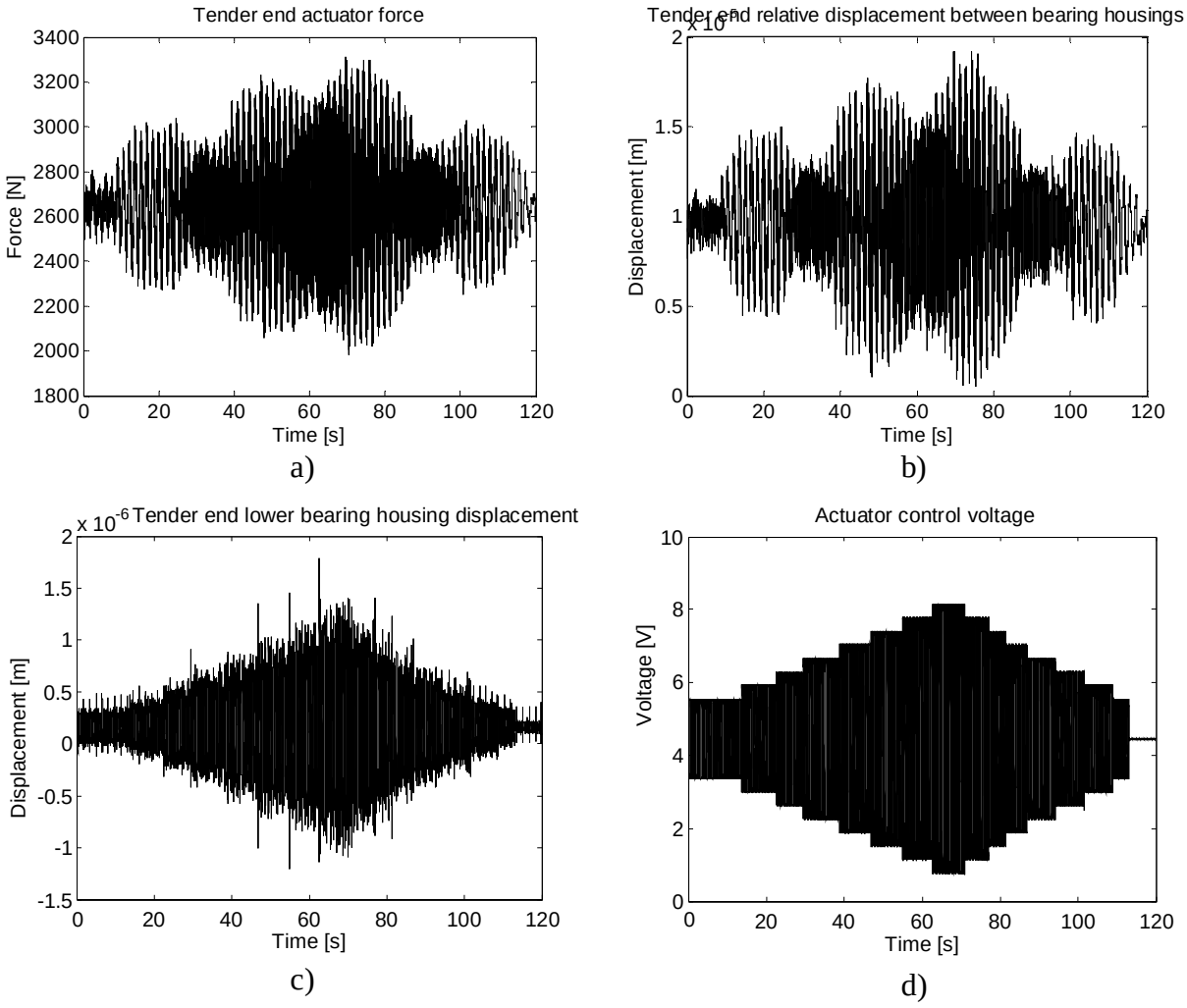

Figure 40. a) TE actuator force, b) TE relative displacement between bearing housings, c) TE lower bearing housing displacement and d) actuator control voltage from amplifier monitoring output.

7.3 Response to varying excitation frequency in the case of damping circuit closed

In Figure 41 the actuator force generation is shown. In the measurements, the actuator driving voltage was *444 V*, amplitude of the control signal *0.7 V* and the excitation frequency of the other actuator was slide in range from *60 Hz* to *200 Hz*.

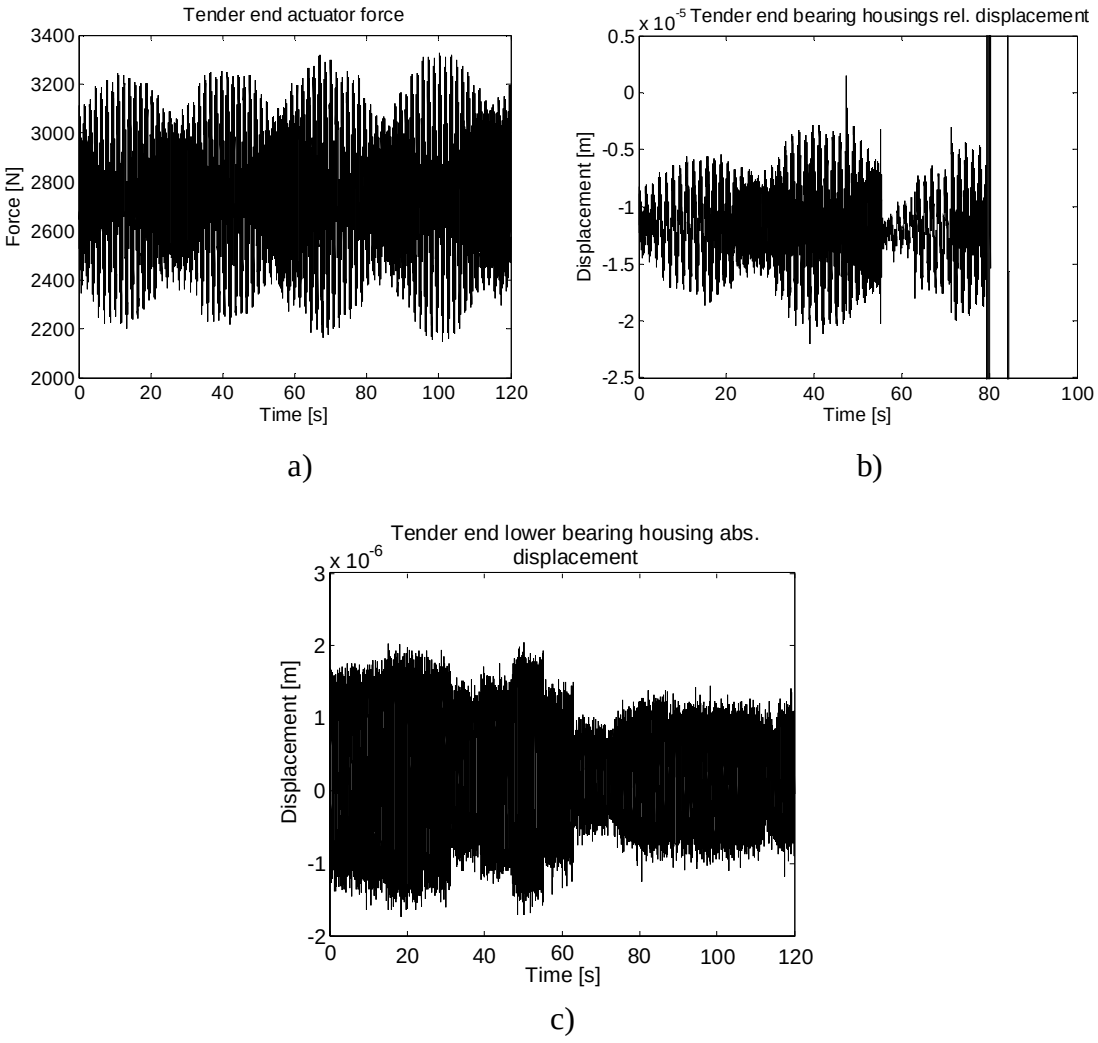

Figure 41. a) TE actuator force, b) TE relative displacement between bearing housings and c) TE lower bearing housing absolute displacement.

The results show that the excitation frequency does not have large influence on the actuator force and relative displacement of the bearing housings.

7.4 Response of tender end to the excitation input at the drive end

In this test the DE piezoelectric actuator was employed as a shaker with frequency of *125 Hz* and amplitude of the control signal *0.8 V*, representing rather strong excitation. In Figure 42 the TE lower and upper acceleration signals are plotted without the

damper. The relative acceleration without the damper is then compared in Figure 43 to the corresponding response with the damper.

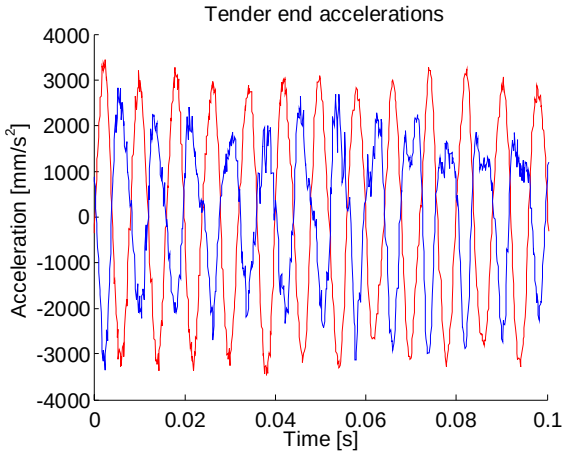

Figure 42. The TE lower and upper acceleration signals without the damper.

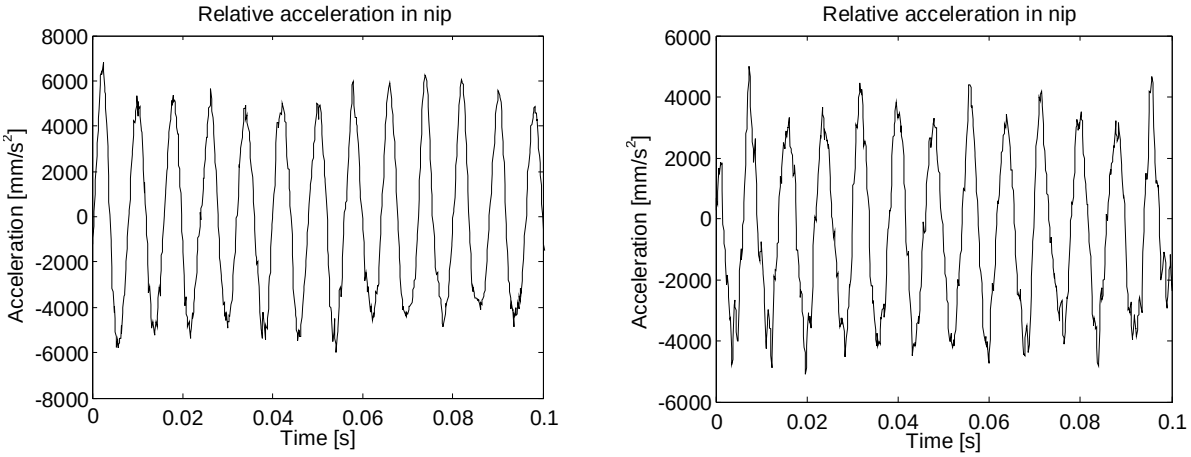

Figure 43. Relative acceleration at TE a) without the damper and b) with the damper.

The spectra of the same signals are shown in Figure 44. In the case of "damper turned on" the derivative gain K_D was set to a value *0.03* which is quite near the instability border of the damper.

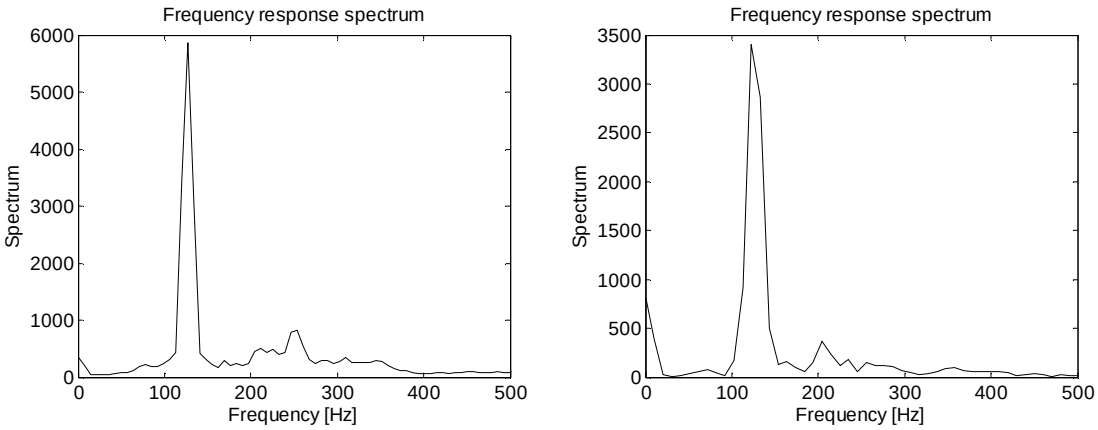

a) b)

Figure 44. Spectra of the relative acceleration signal a) without damper and b) with damper.

From the results one can observe that the vibration at the excited delay-resonance frequency *122 Hz* of the pilot roll press with the damper circuit closed, is clearly lower than in the case in which the damper circuit is open. The output of these tests indicates that the damper circuit is able to damp the relative motion response of the rolls by approximately *40 %*, which is a very promising result.

8. Conclusions

The problem to damp normal oscillations in rolling contact systems has earned considerable interest in the scientific community close to the pulp and paper industry. Non-classical delay-resonances appearing in new polymer-covered rolls have cut production rates in some cases so remarkable that a complete new research line has been opened to find economical solutions to overcome the difficult situation. This is why different approaches and solution strategies have been presented and realized during the last two decades. Although passive, semi-active and smart approaches have been successfully implemented to laboratory and mill scales, there is still one branch aside the mainstream of the research to be declared. This is the use of piezoelectric actuators in an actively controlled damping scheme. This area brings many possibilities and the main purpose of this thesis has been to find out, which methods are the feasible ones and how they should be implemented.

8.1 Analysis of results

A comprehensive literature review has been done on vibration and damping of rolling contact systems and on the use of piezoelectric actuators in various vibration damping and high precise motion control applications. Based on that work, the most promising methods found are the following ones:

(1) Use of the piezoelectric actuators in the position control feedback loop to damp the nip oscillations in the classical D or PD control schemes.
(2) Use of the piezoelectric actuators with an RLC shunt circuit to damp the nip oscillations based on the resonance tuning rules.

A good reason to evaluate these alternative methods has been the similar basis to build the hardware by mechanically connecting the piezoactuators between the bearing units of the two member rolls in the roll stack. In case the rest part of the damping circuit is not working properly, another circuit arrangement can be realized with reasonable costs. The two alternative methods have been in first step evaluated by means of

computer simulations and based on the results the first damping circuit has been also built and implemented under the D control scheme, which is also called the direct velocity feedback approach.

The most important findings of the research work are the following ones:

(1) One not surprising finding in the use of piezoactuators between two bodies in relative vibratory motion is the additional structural stiffness property of the ceramic core and the surrounding metallic casing. This brings some stiffening effect to the relative motion shifting the natural frequencies of the nip oscillation mode higher as well. Such stiffening is normally useful but leads in a rolling contact system to a secondary problem. The geometric imperfections, for instance shape eccentricity or shaft misalignment, are forcing the distance between the rotation centres of the roll bearings to fluctuate, which in turn is bringing a quasistatic component motion and corresponding oscillatory force to the piezoactuator when it tries to damp it. There are practically two possibilities to overcome this problem, which can lead to fatigue damage of the actuator. The first is to make an elastic enough fixing interface for the actuator. This additional motion, however, can use the very limited stroke capacity of the actuator leading to inefficient damping result. Another way is to identify the geometric motion and to compensate this slow error motion by means of a position tracking algorithm superimposed to the primary task to damp the nip oscillations at one decade higher frequency band.

(2) The second finding in the first method alternative is, that not only the structural stiffness of the piezoactuator, but also the control gains are contributing to the cross-coupling stiffness and damping terms in the dynamic equations of motion of the member rolls. This has brought an excellent way to shift the nip oscillation frequency and to adjust the amount of external damping produced by the piezoelectric actuator circuit. Such adaptive tunings can be done even during the process run making it possible to slowly oscillate or in other way to modify the delay-resonance speeds for finding stable running windows.

(3) In the second method to use the RLC shunt circuit, the main finding was that a fixed tuning of the shunt circuit to the natural frequency of the nip system works in principle but the wandering of the frequency under changing process conditions like cover temperature, line load, cover material aging etc. requires an on-line identification system for resonance tracking and based on that also an on-line tuning procedure.

One of the fundamental research questions is the required size of the piezoactuator to produce a sufficient damping result. A common misunderstanding in the vibration damping of heavy objects is the statement to use large powerful actuators. Many examples, for instance the classical dynamic mass damper, show that the counter-effect, when applied at the right phase and early enough, can effectively, even with small actuators, eliminate the initialization of self-excited vibrations, in which category the delay-vibrations also belong. During this thesis work, a series of separate tests has been done, the output of which is that a compact size actuator can effectively work both in shaker and damper services on either ends of the roll stack. If the fixing interface of the stack actuator is stiff enough, the stroke capacity covers easily amplitudes typical for delay driven resonances.

By referring to the research questions stated in chapter 1.2, the main output of this research work can be summarized in the following concluding statements:

(1) The most effective solution for damping purposes is to install the piezoelectric actuators between the bearing housings at both ends of the member rolls to limit the relative normal motion between the rolls. Installation of the actuators parallel with the hydraulic loading actuators between the frame and the lower roll or parallel with the locking cylinder between the frame and the upper roll may lead to an unwanted situation, where only one of the rolls has a stabilized response. The damping of the relative motion requires a coupling mechanism, which allows a free linear motion of the rolls when closing or opening the nip contact while keeping the motion under the piezoelectric control in the locked mode. This hardware interface makes it possible to utilize the structural stiffness of the piezoactuator in a passive way. By connecting the

piezoactuator to an amplifier circuit, a family of different classical controllers, state controllers, counter-force generators or shunt circuits can be flexibly implemented in order to compensate the relative motion between the rolls.

(2) Whirling motions related to imbalance forces and shaft misalignments, or lower harmonics related to the shape imperfections of the member rolls, lead to low frequency oscillatory motion. If the mounting interface is stiff, this motion is heavily loading the piezoactuators. If the interface is too soft, the overloading of the actuators can be avoided, but the price is paid in the performance of the actuators in the damping of the nip oscillations at the frequency band related to the delay-resonances. These difficulties can be avoided by learning-based compensation of the static error sources.

(3) From the family of classical controllers, direct velocity feedback (D control) is the easiest controller to be implemented. If the proportional part is added (PD control), a static compensation block is needed to manage the static error motions. When using external RLC shunt circuit, the tuning of the circuit parameters has to be done on-line to include the dependence of the delay-frequency on the cover temperature and on the line-load level.

8.2 Discussion

Industrial actors have a great interest to invest in a stable enough system, which can be driven without disturbances at broad running speed area. The viscoelastic property of roll covers, however, is still present in many process sections and brings always a risk to high speed paper production lines. This risk can be met by two leading strategies. The first is to make robust and conservative design by means of over-dimensioning the rolls and by using stiff enough primary loading actuator circuits in order to shift the dominating nip oscillation frequency to higher frequency band. If such high cost investment is not possible, piezoelectric damping circuit is always available even as an additional hardware to fix a serious vibration problem in an existing production unit. The performance at high frequency band and a flexible connection to different controllers and electrical damping circuits makes it a competitive alternative among

other damping solutions although the required hardware implementation brings considerable infrastructure costs.

8.3 Further developments

The experimental part of this research work, which includes tedious preparations and modifications of the set-ups, has been done in a limited time-span. This situation forced the focus to the most promising damping strategies based on the classical controllers. For instance, the realization of the RLC circuit and the active vibration damping by generating counter-force effects, have been left for future work. The compensation of the static error motion by learning approach has also been left for further studies.

References

Adachi, K., Awakura, Y., Iwatsubo, T., 2004. Hybrid Piezoelectric Damping for Structural Vibration Suppression, Journal of Intelligent Material Systems and Structures, vol. 15 p. 795, November 2004

Adriaens, H. J. M. T. A. , de Koning, W. L., Banning, R., 2000. Modeling Piezoelectric Actuators, IEEE/ASME Transactions on Mechatronics, vol. 5 no. 4, December 2000

Ahmadian, M., de Guilio, A.P., 2001. Recent Advances in the Use of Piezoceramics for Vibration Suppression, The Shock and Vibration Digest, vol. 33, no. 1, January 2001

Barrett, T.S., Palazzalo, A.B., Kascak, A.F., 1995. Active Vibration Control of Rotating Machinery Using Piezoelectric Actuators Incorporating Flexible Casing Effects, Journal of Engineering for Gas Turbines and Power, vol. 117, January 1995

Behrens, S., Moheimani, S.O.R., 2000. Optimal Resistive Elements for Multiple Mode Shunt Damping of a Piezoelectric Laminate Beam, Proceedings of the 39th IEEE Conference on Decision and Control Sydney, Australia December, 2000

Bradford, R. A., Emmanuel, A. 1988. Calender Vibration Behavior at a Large Newsprint Machine, Appita, 41 (3) May 1988.

Chinn, F. 1999. Dynamic instability of polymer covered press rolls. Pulp & Paper Canada.

Clark, R.L., Saunders, W.R., Gibbs, G.P., 1998. Adaptive structures, Dynamics & Control, Wiley, New York, 1998

Clark, W.W., 2000. Vibration Control with State-Switched Piezoelectric Materials, Journal of Intelligent Material Systems and Structures, Vol. 11, April 2000

Colla, E.L., Piezoelectric Technology for Active Vibration Control, 2008. Internet: www.infoprint.ch/Docs/PiezoelectricTechnology2.pdf (10.5.2008)

Delibas, B., Arockiarajan, A., Seemann, W., 2005. A nonlinear model of piezoelectric polycrystalline ceramics under quasi-static electromechanical loading, Journal of Materials Science: Materials in Electronics, vol. 16, 2005

Emmanuel, A. 1985. Some experiences with calender barring on a newsprint machine and diagnosis of roll corrugations, July 1985, Appita 38 (4).

Filipovic, D., Olgac, N., 1997. Delayed Resonator with Speed Feedback Including Dual Frequency – Theory and Experiments. Proceedings of the 36th Conference on Decicion & Control, San Diego, CA, USA.

Fuller, C.R., Elliot, S.J., Nelson, P.A., 1996. Active Control of Vibration, Academic Press Limited 1996

Genta, G., 2009. Vibration Dynamics and Control, Springer USA 2009

Hagood, N.W., von Flotow, A., 1991. Damping of Structural Vibrations with Piezoelectric Materials and Passive Electrical Networks, Journal of Sound and Vibration, vol. 146 no. 2, 1991

den Hartog, J. P. 1947. Mechanical Vibrations. McGraw-Hill, New York.

Hermanski, M., 1995, Barringbildung am Glättkalander einer Papiermaschine. Das Papier (9): 581.

Johnson, K.L. 1985. Contact Mechanics, Cambridge University Press.

Jokio, M. 1999. Finishing, Papermaking Science and Technology, Book 10, TAPPI Press, Fapet Oy Publ., Helsinki, Finland.

Karhunen, J., Puranen, A., Köliö J., Lehtovirta, E., Hietamäki E. 2005. Method and equipment for attenuation of oscillation in a paper machine or in a paper finishing device. Patent number US 6,911,117 B1, 2005.

Keskinen, E., Kivinen, J.-M., Launis, S., Vikman, K. 1998. Dynamic Analysis of Roll Nip Mechanisms in Papermaking Systems. Proceedings of 10th European Simulation Symposium. SCS, Nottingham. U.K.

Keskinen, E.K., Yuan, L., Järvenpää, V.-M., Launis, S., Cotsaftis, M. 2000. Dynamics of Internal and External Resonances in Rolling Contact of Polymer Covered Rotating Beams. 5th Biennial ASME Conference on Engineering System Design & Analysis, July 10-13, 2000, Montreux, Switzerland.

Keskinen, E.K., Launis, S., and Cotsaftis, M. 2002. Multi-Body Modeling of Paper Calendering Unit by Contact Dynamics Formulation. Gladwell, G.M.L., (Ed.), Contact Mechanics, Ser. in Solid Mechanics and its Appl. (103). Kluwer Academic Publishers, Netherlands.

Kim, J., Varadan, V.V., Varadan, V.K., 1997. Finite Element Modelling of Structures Including Piezoelectric Active Devices, International Journal for Numerical Methods in Engineering, vol. 40, p.817, 1997

Kivinen, J. A. 2001. Variable Parameter Facility for Dynamic Testing of Polymer Covered Paper Machine Rolls. Tampere University of Technology, Publications 347, Doctoral Thesis, ISBN 952-15-0688-1.

Korolainen, T., Kupiainen, S., Puranen, A. 2010. Arrangement for damping vibration in a fiber web machine. Patent number WO2010094834 (A1).

Kustermann, M., 2000, Vibrations in Film Presses. Proc. of TAPPI Coating Conference and Trade Fair, Washington.

Law, H.H., Rossiter, P.L., Simon, G.P., Koss, L.L., 1996. Characterization of Mechanical Vibration Damping by Piezoelectric Materials, Journal of Sound and Vibration, vol. 197 no. 4, 1996

Lehtinen E. 2000. Pigment Coating and Surface Sizing of Paper, Papermaking Science and Technology, Book 11, TAPPI Press, Fapet Oy Publ., Helsinki, Finland.

Moheimani, S.O.R., Fleming, A.J., 2006. Piezoelectric Transducers for Vibration Control and Damping, Springer 2006

Niederberger, D., 2005. Smart Damping Materials using Shunt Control, dissertation to Swiss Federal Institute of Technology (ETH) Zürich, 2005

Nguyen, A.H., Pietrzko, S.J., 2007. Vibroacoustic FE analysis of an adaptive plate with PZT actuator/sensor pairs connected to a multiple-mode, electric shunt system, Finite elements in analysis and design, vol. 43 p. 1120, 2007

Parker, J.A., 1965. Corrugation of Calender Rolls and the Barring of Newsprint, Paper Technology, 6(1), pp. 33-41.

Pasco, Y., Berry, A., 2004. A Hybrid Analytical/Numerical Model of Piezoelectric Stack Actuators Using a Macroscopic Nonlinear Theory of Ferroelectricity and a Preisach Model of Hysteresis, Journal of Intelligent Material Systems and Structures, vol. 15, May 2004

Preumont, A., 1997. Vibration Control of Active Structures, Kluwer Academic Publishers, The Netherlands 1997

Salmenperä, P., 2013. Delay-resonance Control of Roll Press by Speed Variation Approach, Doctoral Thesis, Tampere University of Technology, ISBN 978-952-15-3212-2.

Shelley, S., Zwart, J., Fournier, A. 1997. New Insights into Calender Barring Prevention. Canadian Pulp and Paper Association, Technical Section, Annual Meeting, Montreal, Canada, January.

Simmers, G.E. Jr., Hodgkins, J.R., Mascarenas, D.D., Park, G., Sohn, H., 2004. Improved Piezoelectric Self-sensing Actuation, Journal of Intelligent Material Systems and Structures, vol. 15 p. 941, December 2004

Simões, R.C., Steffen, V. Jr., der Hagopian, J., Mahfoud, J., 2007. Modal Active Vibration Control of a Rotor Using Piezoelectric Actuators, Journal of Vibration and Control, vol. 13, no. 1, 2007

Sueoka, A., Ryu, T., Kondou, T., Tsuda, Y., Katayama, K., Takasaki, K.,Yamaguchi, M., Hirooka, H., 1993. Polygonal Deformation of Roll-Covering Rubber. Transactions of the Japan Society of Mechanical Engineers Series C; Issn:0387-5024; Vol.59; No.563; p. 2078-2085.

Tang, J., Wang, K.W., 2000. High Authority and Nonlinearity Issues in Active-Passive Hybrid Piezoelectric Networks for Structural Damping, Journal of Intelligent Material Systems and Structures, vol. 11 p. 581, August 2000

Töhönen, M., Keskinen, E.K., and Seemann, W. 2011. Damping of Oscillatory Rolling Contact by Piezoelectric Actuators. ASME IMECE2011, November 13-17, 2011, Denver, USA.

Vinicki, J. 2001. Barring Induced Vibration, "Sound and Vibration", Vol. 35, Number 9, 2001.

Virtanen, T. 2006. Fault Diagnostics and Vibration Control of Paper Winders. Dissertation. Helsinki University of Technology.

Vuoristo, T., Kuokkala, V.-T., 2002, Creep, recovery and high strain rate response of soft roll cover materials, Mechanics of Materials, 34 (8), pp. 493-504.

Wang, D., Guo, Z., Hagiwara, I., 2002. Nonlinear Vibration Control by Semi-active Piezo-actuator Damping, JSME International Journal, Series C, vol. 45 no. 2, 2002

Ward, I. M., Hadley, D. W. 1993. An Introduction to the Mechanical properties of Solid Polymers. Wiley, New York.

Yuan, L. 2002. Analysis of Delay Phenomena in Roll Dynamics. Tampere University of Technology, Publications 397, Doctoral Thesis, 2002, ISBN 925-15-0916-3.

Yuan, L., Järvenpää, V.-M., 2009. Nonlinear vibrations in a covered roll system with viscoelastic contact, Communications in Nonlinear Science and Numerical Simulation, 14 (7), pp. 3170-3178.

Zhang, W., Qiu, J., Tani, J., 2004. Robust Vibration Control of a Plate Using Self-sensing Actuators of Piezoelectric Patches, Journal of Intelligent Material Systems and Structures, vol. 15 p. 923, December 2004

Zhou, S., Shi, J., 2001. Active Balancing and Vibration Control of Rotating Machinery: A Survey, The Shock and Vibration Digest, vol. 33 no. 5, September 2001

Tampereen teknillinen yliopisto
PL 527
33101 Tampere

Tampere University of Technology
P.O.B. 527
FI-33101 Tampere, Finland

ISBN 978-952-15-3669-4
ISSN 1459-2045